

## RESEARCH ARTICLE

# Folate receptor 1 is necessary for neural plate cell apical constriction during *Xenopus* neural tube formation

Olga A. Balashova, Olesya Visina and Laura N. Borodinsky\*

## ABSTRACT

Folate supplementation prevents up to 70% of neural tube defects (NTDs), which result from a failure of neural tube closure during embryogenesis. The elucidation of the mechanisms underlying folate action has been challenging. This study introduces *Xenopus laevis* as a model to determine the cellular and molecular mechanisms involved in folate action during neural tube formation. We show that knockdown of folate receptor 1 (Folr1; also known as FR $\alpha$ ) impairs neural tube formation and leads to NTDs. Folr1 knockdown in neural plate cells only is necessary and sufficient to induce NTDs. Folr1-deficient neural plate cells fail to constrict, resulting in widening of the neural plate midline and defective neural tube closure. Pharmacological inhibition of folate action by methotrexate during neurulation induces NTDs by inhibiting folate interaction with its uptake systems. Our findings support a model in which the folate receptor interacts with cell adhesion molecules, thus regulating the apical cell membrane remodeling and cytoskeletal dynamics necessary for neural plate folding. Further studies in this organism could unveil novel cellular and molecular events mediated by folate and lead to new ways of preventing NTDs.

**KEY WORDS:** Folic acid, Neural tube defects, *Xenopus*, Folate receptor

## INTRODUCTION

Neural tube defects (NTDs) are among the most common serious morphological defects diagnosed in human fetuses and newborns with combined incidence of ~1/1000. They result from the failure of the neural tube to close leading to exencephaly or spina bifida (Wallingford et al., 2013). Currently, there is no effective treatment for NTDs once the neural tube has failed to close and, because closure is completed by day 28 of gestation in humans, preventive therapy must be targeted to early pregnancy.

A vast number of clinical studies have established that folate is a prominent environmental factor needed for appropriate neural tube closure (Detrait et al., 2005; MRC Vitamin Study Research Group, 1991; Pitkin, 2007). Low blood folate levels in pregnant women are correlated with higher risk of NTDs in their offspring (Detrait et al., 2005; Smithells et al., 1976) and periconceptional supplementation of folate decreases the recurrence and occurrence of NTDs (MRC Vitamin Study Research Group, 1991).

Folate belongs to the vitamin B family. Folate-derived metabolites are required for DNA, protein and lipid methylation. In particular, folate participates in thymidine and purine synthesis, and is therefore needed for DNA replication and cell division, processes characteristic of rapid growth. Uptake of folate by mammalian cells is mediated by three membrane proteins: reduced-folate carrier, folate receptor [Folr, also called folate binding protein (Folbp)] and the proton-coupled folate transporter (Antony, 1992, 1996; Sirotnak and Tolner, 1999).


The mechanisms by which folate promotes neural tube formation are unclear. The importance of folate uptake systems for the formation of the neural tube has been shown by studies in humans and mice. Significant associations between single-nucleotide polymorphisms (SNPs) in different human folate transporters and myelomeningocele compared with the ethnically paired healthy population have been found, including one SNP in FOLR1, two in FOLR2, five in FOLR3 and two in the reduced folate carrier (O'Byrne et al., 2010). In mice, knockout of *Folr1* results in an open neural tube by embryonic day 9.5, when heterozygotes or wild-type littermate embryos show a closed neural tube. This phenotype leads to death of homozygous embryos *in utero* (Finnell et al., 2002; Piedrahita et al., 1999; Spiegelstein et al., 2004; Wallingford et al., 2013). The specific cellular mechanisms dependent on Folr1 during mouse neural tube formation are unclear.

Whether folate participation in methylation reactions to promote rapid growth is the aspect of folate action necessary for neural tube formation is not completely understood. In humans, a particular mutant variant of methylenetetrahydrofolate reductase, one of the enzymes involved in folate metabolism, has been shown to increase the risk of incidence of NTDs in homozygous infants as well as in homozygous mothers' offspring (Blom et al., 2006; van der Put et al., 1995, 1996), although not every ethnic group studied exhibited this association (Koch et al., 1998; Mornet et al., 1997; Papapetrou et al., 1996; Speer et al., 1997; Wilcken and Wang, 1996). In addition, deficiencies in methylation disturb chick embryo neurulation (Afman et al., 2005, 2003). However, mice in which several enzymes involved in folate metabolism are disrupted do not show NTDs (Chen et al., 2001; Swanson et al., 2001; Watanabe et al., 1995). Moreover, genetic screens in humans showed that there are examples of innate errors in folate metabolism for which NTDs are not over-represented (Blom et al., 2006). Altogether, these studies suggest that the identification of relevant aspects of folate action that influence neural tube formation demands further investigation.

Additional progress in the prevention of NTDs remains on hold owing to the lack of understanding of the basic cellular and molecular mechanisms underlying folate action. *Xenopus laevis* as an animal model is especially suited for investigating events occurring during embryogenesis, because of the ready access to observation and manipulation of early developmental stages. Indeed, it was the pioneer model system from which principles of

Department of Physiology & Membrane Biology and Institute for Pediatric Regenerative Medicine, Shriners Hospital for Children, University of California Davis School of Medicine, Sacramento, CA 95817, USA.

\*Author for correspondence (lnborodinsky@ucdavis.edu)

 L.N.B., 0000-0003-2937-7023

Received 7 March 2016; Accepted 17 February 2017

the process of neurulation were established (Davidson and Keller, 1999; Haigo et al., 2003; Kee et al., 2008; Keller et al., 1992).

Here, we use the *Xenopus laevis* model system to demonstrate that folate promotes neural tube formation by facilitating the changes in neural plate cell shape that are required during neurulation, through a folate receptor-dependent action. The use of this animal model could improve our understanding of the mechanisms of folate action during neural tube formation and, hence, aid in the design of more effective therapies for the prevention of NTDs.

## RESULTS

### Folate receptor 1 is expressed in *Xenopus* embryos during neurulation

Human FOLR1 and its murine homolog Folr1 are primarily found in the placenta, the choroid plexus and the brush border membrane in the kidney (Antony, 1992; Elwood, 1989; Holm et al., 1991; Prasad et al., 1994; Selhub and Franklin, 1984). In the developing mouse embryo, *Folr1* is highly expressed in the yolk sac, neural folds and neural tube (Barber et al., 1999; Saitsu et al., 2003). *Xenopus laevis folr1* has been cloned (accession numbers: BC074206.1; Klein et al., 2002) and shows 80% homology with the human *FOLR1* isoform. Western blot assays with a custom-made antibody against the *Xenopus* protein reveal that Folr1 is readily expressed in mature oocytes and its presence persists throughout development (Fig. 1A,B). Specificity of the antibody was demonstrated by the detection of overexpressed *Xenopus* Folr1 both in immunostained sections from *folr1* mRNA unilaterally injected embryos (Fig. S1A,B) and in western blot assays from *folr1*-flag mRNA-injected embryos (Fig. S1C). Folate is also present in neural plate stage *Xenopus laevis* embryos (stages 13–17; Fig. 1C). Immunostaining of transverse sections from neurulating embryos shows that Folr1 is expressed in the developing neural plate (Fig. 1D,E). Folr1 is enriched in the apical surface of the neural plate, along with C-cadherin (cadherin 3 or blastomere cadherin – Xenbase) (Fig. 1E), in the interectodermal cleft of the two-cell-layered neural plate, and at the boundaries between neural plate and mesoderm (Fig. 1D). In non-neural tissue Folr1 is present in the myocoel and in the notochord lumen (Fig. 1D). These results demonstrate the presence of both Folr1 and folate in *Xenopus* embryos during neural plate folding and neural tube formation.

### Molecular knockdown of folate receptor hinders neural tube closure

To determine whether Folr1 plays a role in *Xenopus* neural tube formation, we used two non-overlapping translation-blocking morpholinos against *Xenopus laevis folr1* sequence (Folr1-MO1 and Folr1-MO2; see Materials and Methods for details) to knock down its expression. Both morpholinos similarly disrupt neural plate folding (Fig. 2A). Results using Folr1-MO1 (hereby referred to as Folr1-MO) are presented for the remainder of the study. Specificity of Folr1-MO was demonstrated by western blot assays from embryos expressing *folr1* mRNA sensitive and insensitive to morpholino inhibition, sense-flag-*folr1* and flag-*folr1*, respectively (see Materials and Methods; Fig. 2B). Folr1-MO does not affect expression of morpholino-insensitive flag-*folr1* mRNA (Fig. 2C, lanes 3 and 4) but reproducibly blocks expression of morpholino-sensitive (sense-flag-*folr1*) mRNA (Fig. 2C, lanes 5 and 6). These results show that downregulation of exogenous Folr1 expression occurs when Folr1-MO targets the sense sequence. However, western blot assay from whole neurulating embryos does not reveal differences in the level of Folr1 expression between control

morpholino (CMO) and Folr1-MO-injected groups (Fig. 2D, lanes 1 and 2). This is possibly due to substantial maternal contribution of Folr1 (Fig. 1B, first lane, oocyte), which might make it impractical to detect the reduction in Folr1 level from downregulation of *de novo* expressed protein in whole-embryo lysates. Nevertheless, a reproducible and significant reduction in Folr1 immunolabeling is apparent in the apical surface of the neural plate when endogenous Folr1 expression is knocked down by Folr1-MO (Fig. 2E,G), suggesting that *de novo* synthesis results in localization of the receptor at the apical neural plate cell surface. In contrast, unilateral injection of CMO does not affect Folr1 expression (Fig. 2F,G). Additionally, knockdown of Folr1 does not result in a significant change in folate levels during neurulation (Fig. 1C), suggesting that Folr1 is not crucial for folate homeostasis during neural tube formation.

We find that knockdown of Folr1 expression in developing *Xenopus* embryos (Fig. 2) impairs neural tube formation and induces NTDs (Fig. 3). The penetrance of the NTD phenotype is approximately 90% (Fig. 3A) and is specific to neurulation as defects in gastrulation are not significantly represented in the Folr1-MO-injected group; there is no delay during gastrulation stages in the Folr1-MO-injected group (mean stage±s.d.: Folr1-MO 11.3±0.3, *n*=131; CMO 10.3±0.1, *n*=66; Folr1-MO+*folr1* mRNA 11.4±0.2, *n*=65), there is no over-representation of apparent gross morphology defects in gastrulating embryos (defective embryos during gastrulation: Folr1-MO 14%, *n*=131; CMO 26%, *n*=66; Folr1-MO+*folr1* mRNA 17%, *n*=65) and there is no significant change in embryo viability during gastrulation (dead embryos: Folr1-MO 11%, *n*=131; CMO 9%, *n*=66; Folr1-MO+*folr1* mRNA 7%, *n*=65). When 20 pmol Folr1-MO are injected the prevalent phenotype (four out of six experiments) is severe, the neural tube is open throughout the anterior-posterior axis, and there is degeneration of neural tissue, apparent as amorphous white tissue protruding from the flanking pigmented non-neural ectoderm in the midline region (Fig. 3A, top middle and bottom left). To rescue the Folr1-MO phenotype, we designed *folr1* mRNA resistant to Folr1-MO inhibition (Fig. 2B; Materials and Methods) that in addition renders a higher level of Folr1 protein expression compared with wild-type mRNA when injected in developing embryos (Fig. 2D, lanes 5 and 6). Western blot assays demonstrate that Folr1-MO downregulates Folr1 expression from wild-type mRNA (Fig. 2D, lanes 3 and 5) but does not affect expression from resistant *folr1* mRNA (Fig. 2D, lanes 4 and 6). The severe phenotype is rescued by restoring Folr1 expression through the injection of resistant *folr1* mRNA (Fig. 3A). In contrast, incubating Folr1-MO-injected embryos with 150 µM folic acid fails to rescue the severe NTD phenotype (Fig. 3A). Embryos exhibiting a severe NTD phenotype do not resist histological procedures due to neuroectoderm degeneration (stage 19), and 100% of them die by the time neural tube closure is complete (stage 21) in sibling control-morpholino-injected embryos. However, in two out of six experiments the majority of embryos did not exhibit the severe phenotype and they survived past stage 19 (*n*=40 Folr1-MO; 30 CMO; 44 Folr1-MO+folic acid). To assess the histological features of the neural tissue caused by Folr1 deficiency, we sectioned Folr1-MO-injected embryos that exhibit a moderate phenotype upon completion of neural tube closure (stage 20–21) in control groups (Fig. 3B). The moderate phenotype consists of incomplete convergence of neural folds in the midline without pronounced degeneration of neural tissue (Fig. 3B, left), which makes these embryos amenable to sectioning and immunohistological procedures. The histological assessment of those experiments with a prevailing moderate

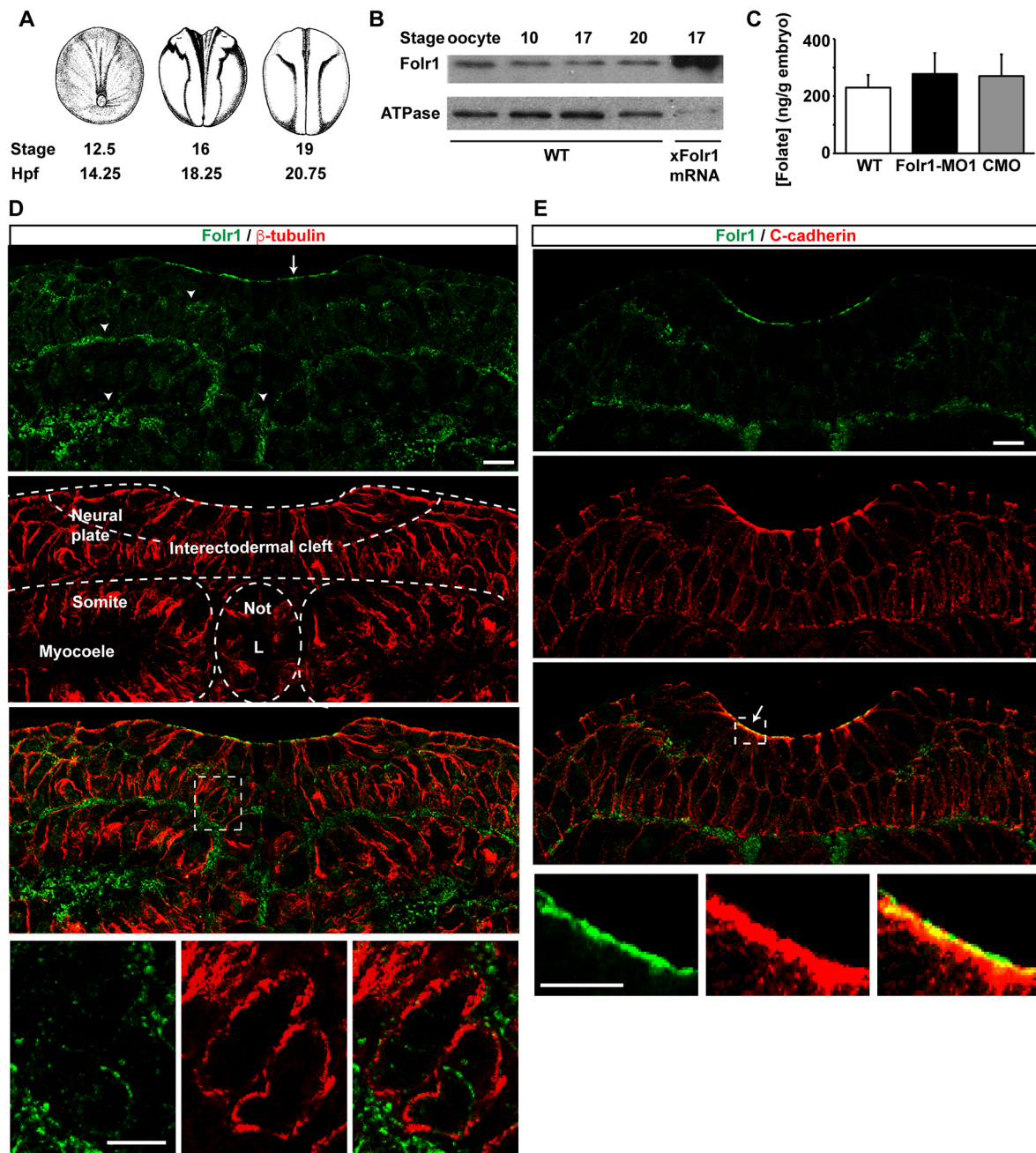


**Fig. 1. Folate receptor 1 expression during *Xenopus laevis* neural tube formation.** (A) Time course of *Xenopus laevis* neurulation. hpf, hours post-fertilization. (B) Western blot assays from homogenates of wild-type (WT) or *Xenopus laevis* folate receptor 1 (Folr1)-overexpressing embryos at the indicated developmental stages. (C) Folate is present during *Xenopus* neural tube formation and folate levels do not change upon Folr1 knockdown. Data show folate levels measured by ELISA assay in homogenates from stage 13–17 (14.5–19 hpf) WT, folate receptor 1 morpholino 1 (Folr1-MO1)- or standard control morpholino (CMO)-injected embryos. Mean  $\pm$  s.e.m.;  $n=8$  independent measurements from  $n>40$  embryos/group; average embryo weight:  $2\pm0.4$  mg. (D,E) Neural plate stage embryos were processed for Folr1 (green) and  $\beta$ -tubulin (D, red) or C-cadherin (E, red) immunostaining. Shown are representative transverse sections of immunostained samples at neural plate stages 15 (D) and 17 (E). (D) Arrow in top panel indicates Folr1 localization at the apical neural plate surface and arrowheads indicate localization in extracellular spaces. Bottom panels show higher magnifications of the boxed area in the panel above and illustrate Folr1 localization to extracellular spaces. L, notochord lumen; Not, notochord. (E) Arrow indicates that Folr1 localizes to the apical neural plate surface along with adherens junction protein C-cadherin. Bottom panels show higher magnifications of the boxed area in the panel above. Scale bars: 20  $\mu$ m.

phenotype shows that most embryos, despite their mildly abnormal overall appearance (Fig. 3B, left), present a defective, spread out and flattened neural tissue with no lumen, even in cases in which the non-neural ectoderm covers up the neural tissue (Fig. 3B). This phenotype is partially rescued by incubating Folr1-MO-injected embryos with folic acid (Fig. 3B), unlike the embryos exhibiting

the severe phenotype, which were only rescued by restoring Folr1 expression (Fig. 3A). These results identify Folr1 as a relevant molecule in the process of *Xenopus* neurulation, in agreement with what has been reported in other model systems (Spiegelstein et al., 2004), and suggest that the interaction between folate and its receptor is necessary for neural tube formation. We ruled out the



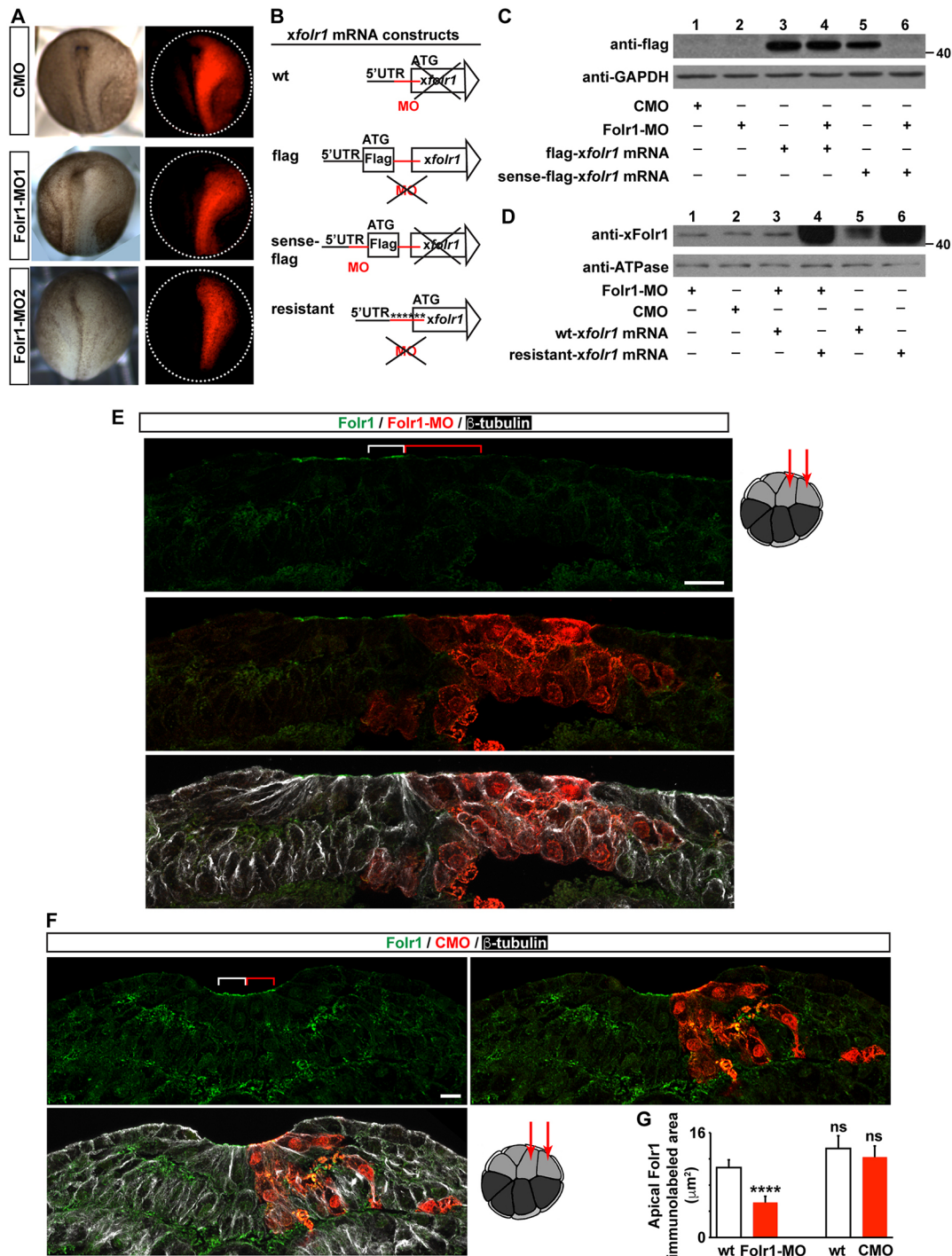


**Fig. 2. Efficacy and specificity of folate receptor 1 knockdown by targeted translation-blocking morpholino.** (A–G) Two- (A,C,D) or sixteen- (E–G) cell-stage embryos were unilaterally (A,E–G) or bilaterally (C,D) microinjected with standard control morpholino (CMO), morpholino against Folr1 (Folr1-MO) and/or with 600 pg Folr1-MO-sensitive (wt-*folr1* mRNA or sense-flag-*folr1* mRNA) or -insensitive *folr1* mRNA (flag-*folr1* mRNA or resistant-*folr1* mRNA). (A) Two non-overlapping Folr1 translation blocking morpholinos (10 pmol/blastomere) elicit similar defects in neural plate folding. Shown are representative examples of unilaterally injected CMO, Folr1-MO1 and Folr1-MO2 embryos. Red indicates morpholino-containing tissue. (B) Schematics of construct design for *folr1* mRNA sensitive and resistant to Folr1-MO. (C,D) Specificity of Folr1-MO. Representative western blot assays for neural plate stage embryos bilaterally injected (10 pmol MO/blastomere) with the indicated constructs and probed with anti-flag (C) or anti-Folr1 (D). GAPDH and Na<sup>+</sup>/K<sup>+</sup> ATPase  $\alpha$ 1 subunit were used as loading controls. (E,F) Representative examples of transverse sections from a neurulating embryo unilaterally microinjected at the 16-cell stage with 1.8 pmol Folr1-MO (E) or CMO (F) per blastomere along with GFP mRNA in the dorsal medial and lateral animal blastomeres, as indicated in drawing on the right, sectioned and processed for Folr1 (green), GFP (red) and  $\beta$ -tubulin (white) immunostaining. Red indicates Folr1-MO- (E) or CMO- (F) containing cells. Scale bars: 20  $\mu\text{m}$ . (E) Folr1-MO downregulates expression of endogenous Folr1 in the neural plate apical surface. Brackets indicate same number of Folr1-MO-containing (red) and wild-type (white) apical neural plate cells. (F) Presence of CMO in medial neural plate cells does not affect Folr1 expression. (G) Graph shows area labeled by apical Folr1 immunostaining in three wild-type and morpholino-containing medial neural plate cells (indicated with brackets in E,F). Mean  $\pm$  s.e.m.;  $n=42$  sections from ten Folr1-MO and CMO unilaterally injected embryos; \*\*\*\* $P<0.0001$ ; ns, not significant; paired and unpaired Student's *t*-tests.



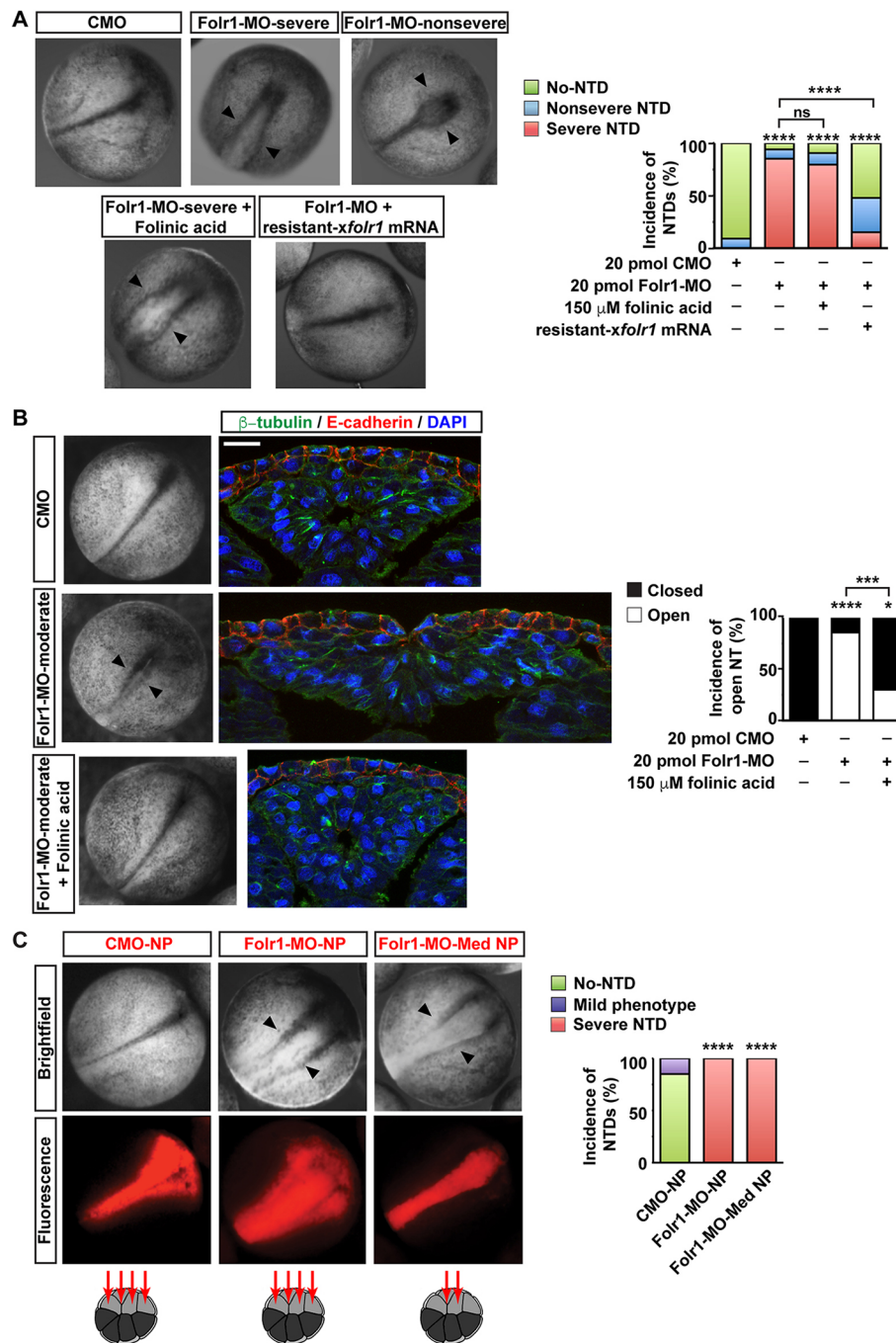


**Fig. 3. Folate receptor 1 knockdown in medial neural plate induces neural tube defects.** (A,B) Two-cell-stage embryos were bilaterally microinjected with standard control morpholino (CMO) or morpholino against *Folr1* (Folr1-MO). Rescue experiments were performed by either microinjecting along with Folr1-MO, 250 pg *folr1* mRNA resistant to Folr1-MO (resistant-*folr1* mRNA) or by incubating Folr1-MO-injected embryos with 150  $\mu$ M folinic acid (FA). (A) Representative examples of control and experimental sibling embryos during neural tube closure (20 hpf) from four out of six experiments in which the severe NTD phenotype prevails in Folr1-MO-injected embryos. Arrowheads indicate open neural tube. Graph shows incidence of severe and nonsevere defective neural tube. Mean $\pm$ s.e.m.; (number of embryos): 20 pmol CMO (89), 20 pmol Folr1-MO (68), 20 pmol Folr1-MO+150  $\mu$ M FA (54), Folr1-MO+*folr1* mRNA (46); \*\*\*\* $P$ <0.0001; ns, not significant; two-tailed Mann-Whitney U-test (Wilcoxon rank-sum test). (B) Folr1-MO-induced moderate NTD phenotype results in open neural tube. Shown are representative examples of whole embryos at stage 21 and transverse sections of the neural tissue from Folr1-MO-injected embryos exhibiting a moderate NTD phenotype (arrowheads; two out of six experiments) and their siblings injected with CMO or Folr1-MO and FA. Embryos were then processed for  $\beta$ -tubulin (green) and E-cadherin (cadherin 1; red) immunostaining and nuclear labeling (blue, DAPI). Graph shows percentage of embryos with open neural tube; number of embryos: CMO (21), Folr1-MO (21), Folr1-MO+FA (20); \*\*\*\* $P$ <0.0001, \*\*\* $P$ <0.0005, \* $P$ <0.01; Mann-Whitney two-tailed U-test (Wilcoxon rank-sum test). (C) Dorsal medial and lateral (medial+lateral neural plate, NP) or only dorsal medial (medial neural plate, Med NP) animal blastomeres from 16-cell-stage embryos were microinjected with 3 pmol/blastomere CMO or Folr1-MO along with Alexa 594-dextran conjugate (in red). Embryos were fixed and photomicrographed under a macroscope. Red indicates CMO- or Folr1-MO-containing tissue. Graph shows incidence of severe NTD phenotype (%). Number of embryos with severe neural tube defects out of total in each group was: 0/33 CMO-NP, 42/42 Folr1-MO-NP and 44/44 Folr1-MO-Med NP; \*\*\*\* $P$ <0.0001; Mann-Whitney two-tailed U-test (Wilcoxon rank-sum test).

possibility that Folt1-MO was inducing neural plate cell death by assessing number of apoptotic cells during neural plate folding, a developmental period in which apoptosis is negligible in the neural tissue (Hensey and Gautier, 1998; Sugimoto et al., 2007). Results show that there are no apoptotic cells in Folt1-MO-containing or contralateral neural plate (Fig. S2A).

### **Folate receptor localized in the superficial neural plate is necessary for the apical constriction of neural plate cells and is required for neural plate folding**

To assess whether the effect of folate is tissue specific, Folt1-MO was targeted to neural plate cells by injecting 1.8–3 pmol Folt1-MO into the dorsal medial and dorsal lateral animal blastomeres of 16-cell-stage embryos (Wallingford and Harland, 2002). Results show that knocking down Folt1 in neural tissue disrupts neural tube formation in 100% of the embryos whereas injection of CMO does not affect neurulation in most embryos and only induces a mild phenotype in 15% of them (Fig. 3C). Transverse sections of Folt1-MO unilaterally injected embryos in target tissues reveal that downregulation of Folt1 expression in the neural plate perturbs its folding (Fig. 2E). In contrast, knockdown of Folt1 in non-neural tissues, such as the mesoderm and non-neural ectoderm (Fig. S3), or injection of CMO in neural tissue (Fig. 2F) does not affect neural plate folding, indicating that Folt1 expression in the neural plate is necessary to promote neural tube formation and that Folt1 knockdown in neural plate only is sufficient to induce NTDs.

Injection of the 16-cell-stage dorsal medial or dorsal lateral animal blastomeres renders a neural plate with primarily medial or lateral affected cells, respectively (Wallingford and Harland, 2002). Embryos with Folt1-MO-containing medial neural plate cells exhibit 100% incidence of NTD phenotype (Fig. 3C). Moreover, results show that apical constriction of cells from the superficial layer of the medial neural plate is deficient in morphant cells compared with cells in the contralateral wild-type side (Fig. 4A–C). This leads to wider apical surface at the midline that hinders folding of the neural plate (Fig. 4A–C). In contrast, cellular defects when lateral neural plate cells are targeted are not apparent and the overall morphogenesis of the neural tube is not compromised (Fig. 4D). To measure quantitatively and dynamically the impairment of apical constriction of medial neural plate cells resulting from knocking down Folt1, we time-lapse imaged the apical surface of the neural plate during stages of neural plate folding (from stage 15–15.5 to stage 16.5–17) in Folt1-MO- and CMO-unilaterally injected live embryos expressing membrane-GFP. The data show that Folt1-MO-containing cells fail to reduce their apical surface over time (change in apical surface:  $17 \pm 12 \mu\text{m}^2/\text{h}$ , mean  $\pm$  s.e.m.,  $n=30$  cells) whereas CMO-containing and contralateral wild-type cells in CMO or Folt1-MO embryos exhibit a rate of surface reduction of  $84 \pm 9$ ,  $105 \pm 10$  and  $103 \pm 13 \mu\text{m}^2/\text{h}$  (mean  $\pm$  s.e.m.,  $n=30$  cells from five embryos/group), respectively, during neural plate folding (Fig. 5; Movies 1 and 2). We did not include dividing superficial neural plate cells (Movie 3) in the apical surface measurements to exclude the effect of cell division on cell surface reduction during neural plate folding. Folic acid deficiency is known to inhibit cell proliferation. Hence, it may be argued that Folt1 knockdown might induce neural tube defects by impairing cell division. However, in *Xenopus laevis* neural tube formation proceeds even when cell division is inhibited (Harris and Hartenstein, 1991). In agreement with this, our data show that only a small number of neuroepithelial superficial cells undergo division (wild type:  $2 \pm 0.5\%$  per 1 h of neurulation, mean  $\pm$  s.e.m.), whereas all neuroepithelial cells in the superficial layer exhibit apical constriction (Fig. 5; Movie 2). Nevertheless, similar

numbers of dividing cells are apparent in wild-type, Folt1-MO- and CMO-containing superficial neural plate (Folt1-MO:  $1 \pm 0.5\%$ , CMO:  $0.9 \pm 0.6\%$  dividing cells/h, mean  $\pm$  s.e.m.). These results suggest that expression and function of Folt1 in medial neural plate cells during neurulation is necessary for medial cell apical constriction.

To determine the early targets of Folt1 deficiency leading to impaired apical constriction, we examined actin dynamics in the superficial neural plate during initial constriction. We failed to find any significant differences between actin dynamics in superficial medial neural plate cells containing Folt1-MO and their wild-type counterparts (Fig. S4A). Similarly, localization of apical proteins, such as the tight junction component ZO-1 is comparable in wild-type and Folt1-MO-containing cells (Fig. S4B). These results suggest that regulation of actin dynamics or establishment of overall apicobasal polarity are not initial mechanisms of Folt1 action.

Remodeling of adherens junctions between cells is crucial for tissue morphogenesis (Nishimura and Takeichi, 2009; West and Harris, 2016). C-cadherin is an important component of adherens junctions in *X. laevis* neural plate (Nandadasa et al., 2009). Apical Folt1 in the neural plate partially colocalizes with the adherens junction component C-cadherin and its molecular partner  $\beta$ -catenin (Fig. 6A). Moreover, both C-cadherin and  $\beta$ -catenin co-immunoprecipitate with Folt1 (Fig. 6B). Altogether, these results indicate molecular interaction between Folt1 and prominent cell adhesion and cytoskeleton organizer molecules in the apical surface of medial neural plate cells. C-cadherin endocytosis is required for morphogenic movements in gastrulating *Xenopus* embryo (Jarrett et al., 2002). We find that neural plate cells undergoing apical constriction contain C-cadherin-immunopositive puncta associated with early endosomes (Eeal-immunopositive vesicles; Mu et al., 1995; Fig. S5), which indicates that C-cadherin endocytosis occurs during apical constriction. Indeed, reduction of the apical surface in constricting cells (Fig. 5) requires internalization of apically localized C-cadherin. Folt1 knockdown in the medial neural plate is accompanied by a decrease in the number of C-cadherin-containing endosomes in superficial cells (Fig. 6C). This effect does not appear to be an overall disruption of endocytosis but specific to C-cadherin compartmentalization, as total number of Eeal-immunopositive vesicles is comparable in Folt1-MO and CMO-containing medial neural plate cells. In contrast, total C-cadherin-containing internal vesicles are markedly reduced in Folt1-deficient cells (Fig. 6C). Altogether, these results suggest that Folt1 interacts with cell adhesion and cytoskeletal machinery responsible for medial neural plate cell apical constriction. This interaction appears to be necessary for regulating trafficking of cadherins.

### **Pharmacological inhibition of folate uptake systems induces neural tube defects**

Pharmacological inhibition of folate action in developing *Xenopus* embryos allows for better temporal resolution of the perturbation and assessment of neural tube formation dynamics. Results show that incubation of *Xenopus* embryos with methotrexate (MTX), a widely used folic acid uptake inhibitor (Jolivet et al., 1983), from the moment neurulation begins, perturbs neural tube formation. This effect is dose dependent with a threshold at  $10 \mu\text{M}$  (Fig. 7). We can conclude that the effect of MTX is due to inhibition of folic acid action because preincubation of embryos with 1–10 mM folic or folinic acid rescues the MTX-induced phenotype (Fig. 7). We ruled out the possibility that MTX treatment during the process of

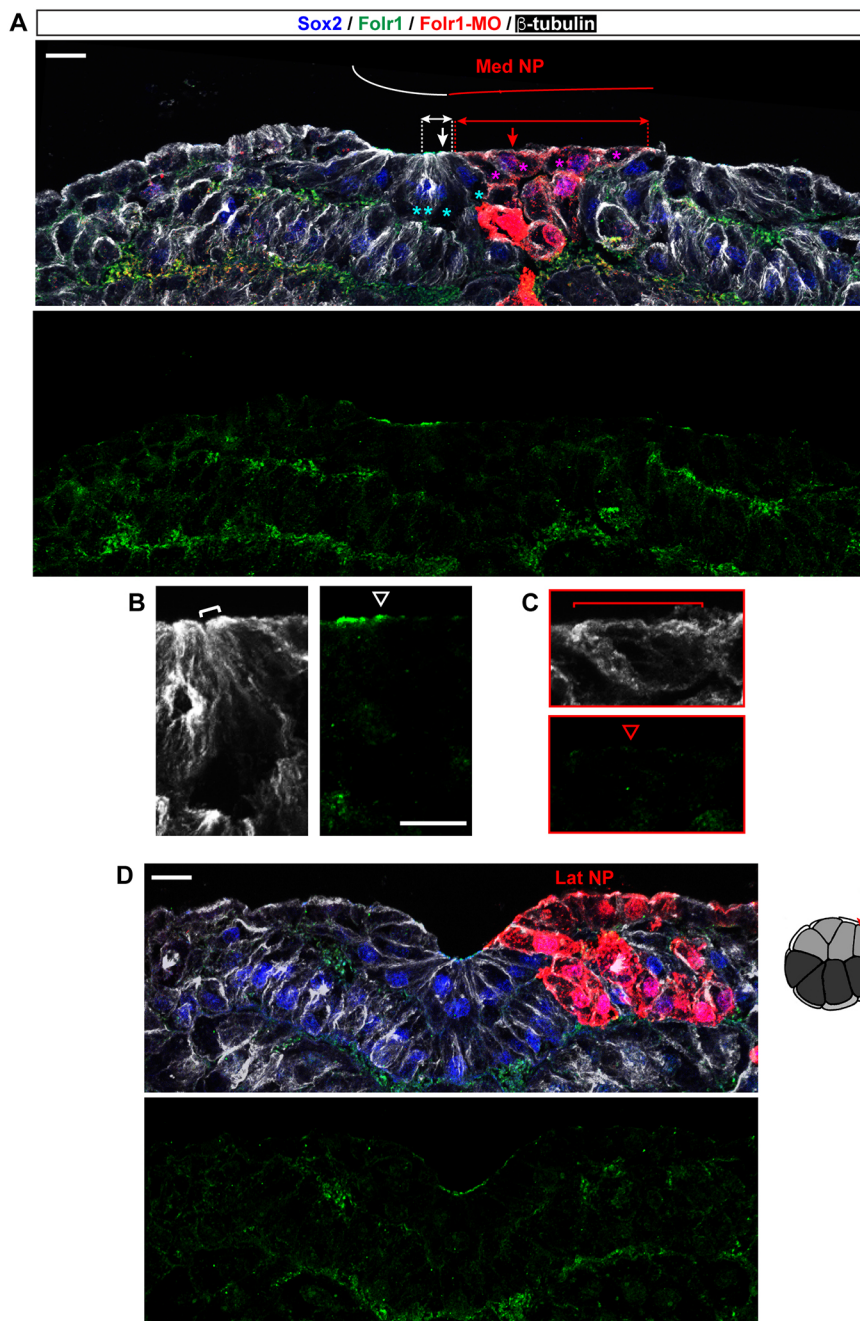


**Fig. 4. Folate receptor 1 in medial neural plate cells is necessary for changes in cell morphology required for neural plate folding.**

(A–D) Representative examples of neurulating embryos unilaterally microinjected at the 16-cell stage with 1.8 pmol Follr1-MO along with GFP mRNA in the dorsal medial (A–C) or dorsal lateral (D) animal blastomeres, as indicated in drawings on the right, sectioned and processed for Sox2, neural progenitor marker (blue), Follr1 (green), GFP (red) and  $\beta$ -tubulin (white) immunostaining. Red indicates Follr1-MO-containing cells. (A) Follr1 knockdown in medial neural plate (Med NP) cells impedes neural plate folding. Asterisks indicate same number of medial cells in wild-type (blue) and Follr1-deficient (pink) sides of the neural plate counted from the midline to represent the impact on the extent of the medial apical surface (white and red double arrows). Curves indicate the bending of the neural plate in wild-type (white) and Follr1-deficient (red) tissues. Arrows in A indicate cells shown in B (white, wild type) and C (red, Follr1 deficient). (B) Wild-type apically constricted (bracket) cell (second from the midline) from the superficial layer of the medial neural plate. Arrowhead indicates apically localized Follr1. (C) Cell (second from the midline) from the superficial layer of the Follr1-deficient side (red) of the medial neural plate fails to constrict (bracket). Arrowhead indicates lack of apically localized Follr1. (D) Follr1 knockdown in lateral neural plate (Lat NP) cells does not induce any apparent morphogenic phenotype. Scale bars: 20  $\mu$ m.

neurulation has a cytotoxic effect on neural plate cells by assessing number of apoptotic cells. Results show that there are no apoptotic neural plate cells during neurulation in control or MTX-treated embryos (Fig. S2B).

We assessed the effect of three lipophilic methotrexate analogs that also inhibit dihydrofolate reductase (DHFR) but, unlike MTX, do not affect folate interaction with the folate receptor or carrier (Grem et al., 1994; Hook et al., 1986; Zimmerman et al., 1987). Chemotherapeutic efficacy and DHFR inhibitory effect of the drugs have been demonstrated *in vitro*, in human colon and Chinese hamster ovary cancer cells and in mouse leukemia cells, and *in vivo*, in mice inoculated with leukemia cells and in rat intestine (Grem et al., 1994; Hook et al., 1986; Zimmerman et al., 1987). Results show that none of the lipophilic DHFR inhibitors, used at saturating doses, induces NTDs (Fig. 7). Our findings suggest that MTX-

induced NTDs are due to interference with the interaction between folate and its uptake systems and not with folate metabolism.

## DISCUSSION

This study introduces *Xenopus laevis* as an instrumental system for investigating the mechanisms of folate action during neurulation. Our findings identify a novel role of folate and its receptor in regulating changes in neural plate cell morphology, which are necessary for appropriate neural tube formation. The fact that folate action is relevant for neural tube formation in human, mouse, chicken, zebrafish and frog argues for both a conserved function of this molecule and conserved mechanisms of neurulation. Although folate is known as an essential co-factor that supports rapid growth by enabling DNA and amino acid synthesis, in *Xenopus laevis*, unlike mammals and birds, cell proliferation is



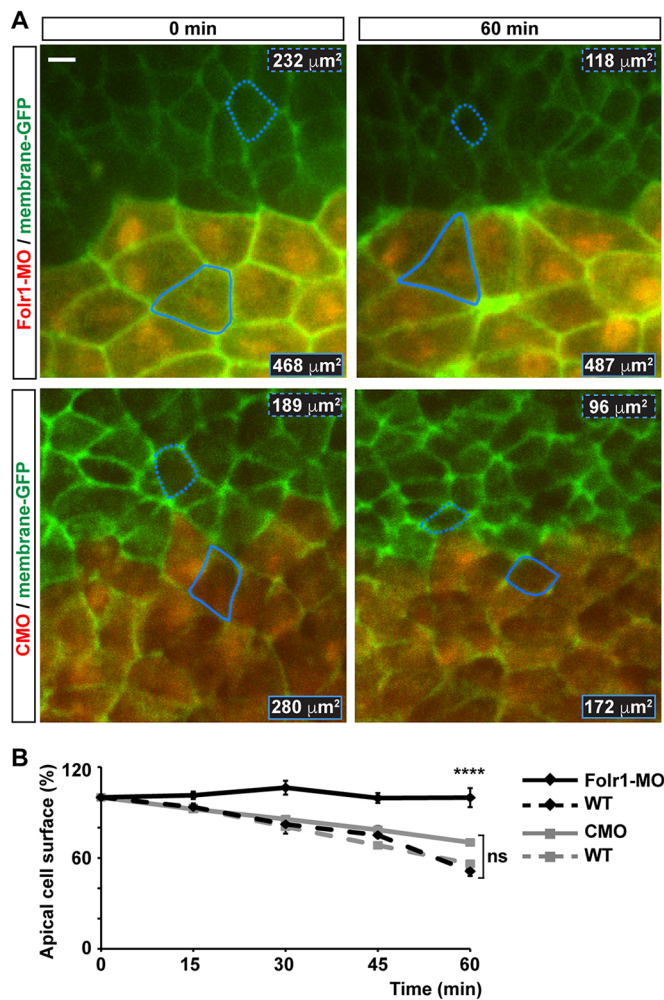


**Fig. 5. Medial neural plate cells deficient in folate receptor 1 fail to constrict apically during neural plate folding.** Two-cell-stage embryos were unilaterally microinjected with 10 pmol morpholino against Folr1 (Folr1-MO) or control morpholino (CMO) along with Alexa Fluor 594-dextran conjugate and bilaterally injected with membrane-GFP. Apical surface of superficial neural plate was time-lapse imaged from whole embryos at a rate of  $0.2 \text{ min}^{-1}$ . Regions of interest were selected to contour cells close to the midline that remained visible during the 1-h recording and did not divide during this period. (A) Shown are representative examples for the indicated time points of Folr1-MO- and CMO-unilaterally injected and imaged embryos. Outlined is one wild-type (dashed) and one MO-containing (solid) cell for which the apical surface was measured over time. Numbers indicate apical cell surface for the same outlined cells at 0 and 60 min of recording. Scale bar: 10  $\mu\text{m}$ . (B) Graph shows apical cell surface (as percentage of initial cell surface at 0 min, 100%) at the indicated time points. Mean  $\pm$  s.e.m.;  $n=30$  Folr1-MO-, 28 CMO-containing cells, and 30 contralateral wild-type (WT) cells per group; \*\*\*\* $P<0.0001$ ; ns, not significant; two-way ANOVA.

not necessary for neural tube formation; *Xenopus* embryos undergo neurulation even when DNA synthesis is blocked (Harris and Hartenstein, 1991). Nevertheless, interfering with folate action induces NTDs in this species, arguing for a previously unidentified role of folate during neural tube closure. Hence, this model system provides the opportunity to determine novel mechanisms triggered by folate action. Indeed, we find that inhibiting one of the most important enzymes of folate metabolism using analogs of methotrexate that bypass the uptake systems due to their lipophilic nature (Grem et al., 1994; Hook et al., 1986; Zimmerman et al., 1987), does not induce NTDs, unlike

methotrexate, suggesting that folate interaction with its receptor is relevant for the formation of the neural tube besides its action as a vitamin and growth-promoting factor.

Despite the fact that apoptosis is not apparent during neural plate folding in embryos deficient in folate receptor, in the majority of Folr1-MO-injected embryos strong neural tissue degeneration occurs at later neurulation stages, indicating that, ultimately, neural cell death takes place as a result of Folr1 downregulation. Although the mechanisms responsible for neural tissue degeneration remain to be elucidated, one possibility is that interfering with folate receptor action results in the observed disruption of trafficking of apical cell adhesion proteins such as C-cadherin, the major cadherin present during *Xenopus laevis* early neurulation (Nandadasa et al., 2009), disturbing the necessary dynamics of cell-cell attachment and impeding neural plate cell apical constriction, as shown in this study. In this context, it is possible that prolonged exposure of embryonic neural tissue to the external saline might cause degeneration. This scenario resembles the two-hit-pathogenesis model for human neural tube defects in which the open neural tube is the first hit followed by *in utero*-acquired neural tissue destruction as the second hit (Meuli and Moehrlen, 2014).

This study identifies the neural tissue as the main target of folate action during neural tube formation. Neural plate cells are prominently engaged during neurulation and their change in cell morphology is crucial for shaping of the neural plate and closing of the tube (Colas and Schoenwolf, 2001; Moury and Schoenwolf, 1995; Ossipova et al., 2014; Schoenwolf, 1988; Schoenwolf et al., 1989). We find Folr1 colocalized at the apical membrane of superficial neural plate cells with C-cadherin and  $\beta$ -catenin. Apically localized molecules play crucial roles during neural plate folding as scaffolding proteins that participate in the apical constriction of cells (Eom et al., 2011; Haigo et al., 2003; Hildebrand and Soriano, 1999; Morita et al., 2010; Nandadasa et al., 2009; Nishimura and Takeichi, 2008; Ossipova et al., 2014). For example, cadherins coordinate the cytoskeletal dynamics and cell-cell interactions necessary for tissue bending and morphogenesis (Nishimura and Takeichi, 2009; West and Harris, 2016). We discovered a molecular interaction among Folr1, C-cadherin and  $\beta$ -catenin. Apical constriction requires spatiotemporal regulation of apical membrane remodeling, which in turn depends on timely endocytosis of apical membrane components (Lee and Harland, 2010). The polarized localization of Folr1 in neural plate cells during neural tube formation contributes to the neural tube morphogenic process by enabling medial neural plate cell apical constriction, potentially through the regulation of C-cadherin trafficking. The results from this study focus the research field on the neural tissue and the process of neural tube formation as specific targets of folate action and argue for considering more specific roles of the vitamin folate on nervous system development and function. Intriguingly, it has been shown that folate improves axonal regeneration after spinal cord and sciatic nerve injury by an upregulation of Folr1 expression (Iskandar et al., 2010) and supplementation of pregnant rats with a high folate diet alters synaptic transmission and seizure susceptibility in their offspring (Giroto et al., 2013). A recent study shows that the presence of folate receptor-blocking antibodies during gestation and pre-weaning in rats disturbs adult social behavior of offspring (Sequeira et al., 2016), in agreement with the association between folate receptor autoantibodies found in children suffering from the infantile-onset cerebral folate deficiency, who exhibit neuropsychiatric and neurologic manifestations (Ramaekers et al., 2005).

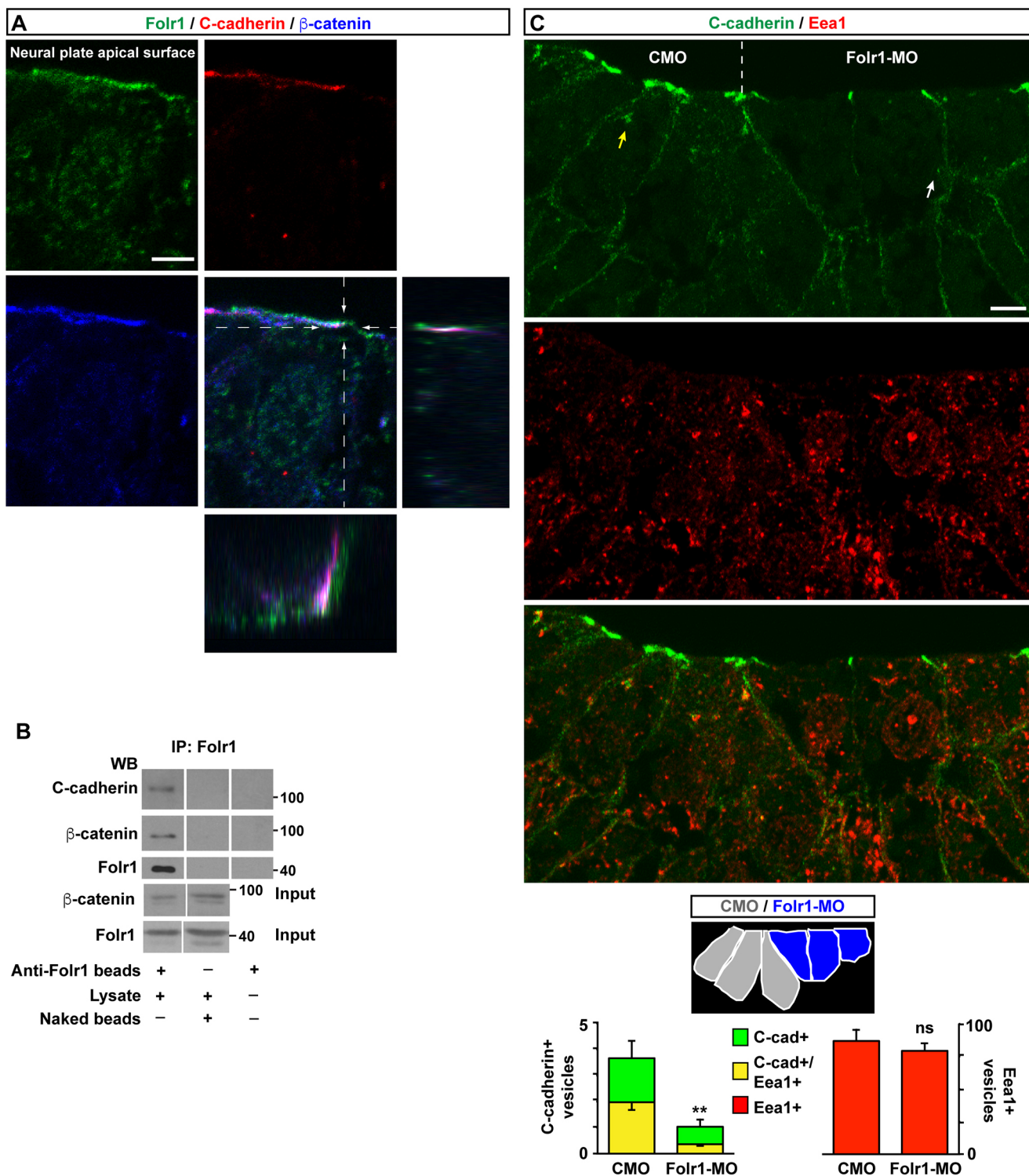


**Fig. 6. Folate receptor interacts with C-cadherin and is necessary for its endocytosis in medial neural plate cells during neural plate folding.** (A) Neural plate stage embryos were processed for Folr1 (green), C-cadherin (red) and  $\beta$ -catenin (blue) immunostaining. Shown is a representative transverse single z-section of immunostained stage 15 medial neural plate cell with orthogonal view through the indicated planes to demonstrate partial apical colocalization of Folr1, C-cadherin and  $\beta$ -catenin in the neural plate. Scale bar: 5  $\mu$ m. (B) C-cadherin and  $\beta$ -catenin co-immunoprecipitate with Folr1. Lysates from wild-type neural plate stage embryos were incubated with anti-Folr1-crosslinked beads or naked beads. Co-immunoprecipitated proteins were dissociated from beads and run in SDS-PAGE gels for western blot assays with anti-Folr1, C-cadherin and  $\beta$ -catenin antibodies. Shown are representative western blot assays, which were performed five times with similar results. (C) The number of C-cadherin-containing vesicles including C-cadherin-containing early endosomes is reduced in Folr1-deficient medial neural plate cells. Two-cell-stage embryos were unilaterally microinjected with CMO and Folr1-MO in contralateral blastomeres. Shown is a representative example of transverse section from a neurulating embryo immunostained for C-cadherin (green) and Eea1 (red). Schematic indicates the cells from which the number of immunopositive vesicles were counted. Yellow arrow points to a C-cadherin<sup>+</sup>/Eea1<sup>+</sup> vesicle and white arrow points to a C-cadherin<sup>+</sup>/Eea1<sup>-</sup> vesicle. Scale bar: 10  $\mu$ m. Graph shows mean $\pm$ s.e.m. C-cadherin- and EEA1-labeled vesicles/cell measured in 54 CMO- and 54 Folr1-MO-containing medial neural plate cells in 18 sections from five embryos; \*\*P<0.005; paired Student's t-test.



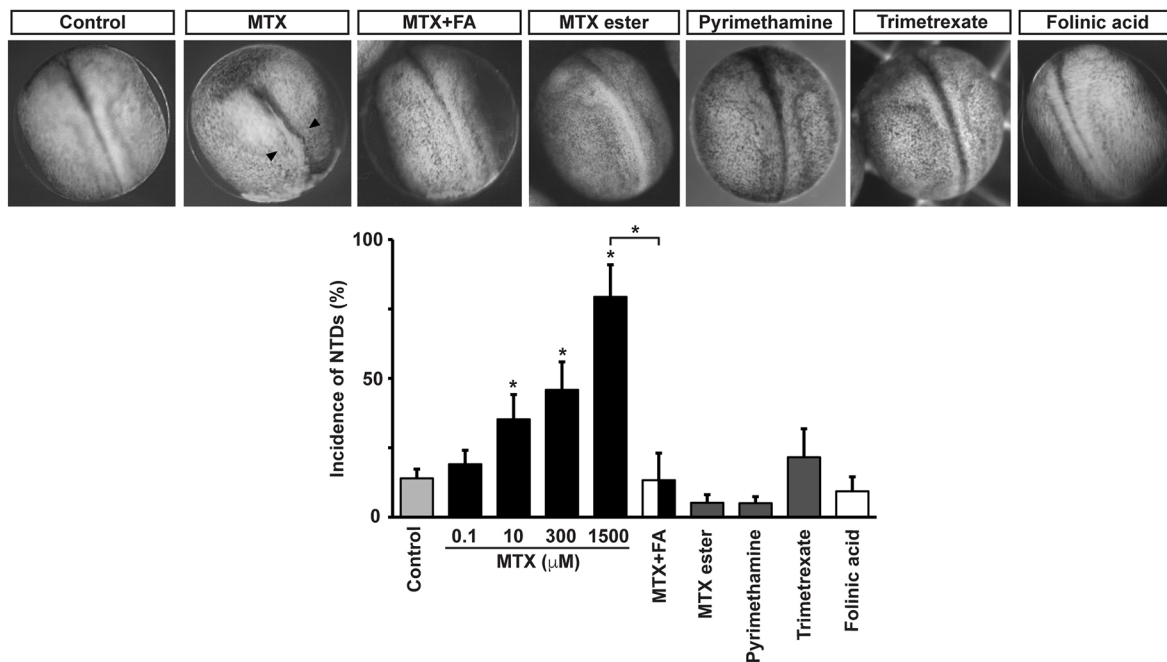


**Fig. 7. Pharmacological inhibition of folate uptake systems affects *Xenopus laevis* neural tube formation.** Embryos at stage 13 (14.75 hpf) were incubated with 100 nM–1.5 mM methotrexate (MTX), 1 nM–300 μM methotrexate ester, 1 nM–100 μM pyrimethamine, 100–500 μM trimetrexate or vehicle (control, 0.3% DMSO or saline). Embryos were fixed and photographed under a macroscope when controls reached neural tube closure, at stage 20 (22 hpf). Shown are representative examples. Arrowheads indicate defective neural tube closure. Rescue of 1.5 mM MTX-induced NTD phenotype was performed by preincubating two- to four-cell-stage embryos with 10 mM folinic acid (FA). Graph shows mean±s.e.m. percentage defective embryos;  $n \geq 6$  independent experiments with  $n \geq 10$  embryos per group, per experiment; \* $P < 0.01$ ; two-way ANOVA.

Future studies are needed to elucidate further the cellular and molecular mechanisms underlying folate action during nervous system development, which will contribute to the development of effective therapies to prevent neural tube defects.

## MATERIALS AND METHODS

### Frog embryos

Mature oocytes were collected from a female frog previously injected with human chorionic gonadotropin and placed in a dish with a small piece of minced testis. This is considered time 0 of fertilization. Fertilized oocytes were kept in 10% MMR saline, containing (in mM): 10 NaCl, 0.2 KCl, 0.1 MgSO<sub>4</sub>, 0.5 HEPES, 5 EDTA and 0.2 CaCl<sub>2</sub>. De-jellying of embryos was performed by briefly swirling fertilized eggs in 2% cysteine solution, pH 8. Developmental stages were recorded according to Nieuwkoop and Faber (1994). Animals were handled according to Institutional Animal Care and Use Committee guidelines using humane procedures to prevent animal suffering.

### Western blot assays

Crude membrane fraction was obtained from non-fertilized eggs, stage 10, 17 and 20 embryos (ten embryos for each group) to assess endogenous expression of folate receptor 1 (Folr1). Briefly, embryos were homogenized in 20 mM Hepes pH 7.4, 1 mM EDTA, 1 mM EGTA, protease inhibitors cocktail (784115, Thermo Fisher Scientific) on ice and centrifuged for 10 min at 1000 *g*. Supernatant was then centrifuged at 16,100 *g* for 30 min. Pellets of crude membrane fraction were resuspended in 2× protein loading buffer [125 mM Tris-HCl, pH 6.8, 4% SDS, 20% (w/v) glycerol, 0.005% Bromophenol Blue]. PVDF membrane was probed with anti-Folr1 rabbit polyclonal affinity-purified antibody raised against the peptide KHQKVDPGPEDDLHC (custom made by GenScript), 1:500 in 5% milk followed by incubation with horseradish peroxidase (HRP)-conjugated secondary antibody (711-035-152, Jackson ImmunoResearch; 1:10,000) and visualized by Western Lightning Plus-ECL, Enhanced Chemiluminescence Substrate (NEL103E001, Perkin Elmer).

PVDF membranes were stripped in 0.2 M glycine HCl buffer, pH 2.5, 0.05% Tween for 20 min and re-probed with anti-α1 subunit of Na<sup>+</sup>/K<sup>+</sup>

ATPase antibody (ab767, Abcam), plasma membrane marker, 1:1000 in 5% bovine serum albumin. To assess exogenous flag-tagged Folr1 expression, eight stage-17 embryos injected with 600 pg flag-*folr1* mRNA at the two-cell stage were homogenized in extraction buffer containing 1% Triton X-100, 150 mM NaCl, 25 mM Tris pH 7.4, 1 mM EDTA, 1 mM EGTA and protease inhibitors cocktail. Samples were centrifuged at 16,100 *g* for 10 min and pellet discarded. Supernatant was processed as described above and immunoblotted with primary anti-flag mouse antibody (MA1-91878, Thermo Fisher Scientific; 1:500), then re-probed with GAPDH antibody at 1:20,000 (sc-47724, Santa Cruz Biotechnology) as protein loading control.

### Co-immunoprecipitation

Fifteen neurulating embryos were homogenized in extraction buffer containing 1% Triton X-100, 150 mM NaCl, 25 mM Tris pH 7.4, 5 mM EDTA, protease inhibitor cocktail (78415, Thermo Fisher Scientific) on ice. Insoluble proteins were pelleted by centrifugation at 16,100 *g* for 10 min. Folr1 was immunoprecipitated from the soluble fraction overnight at 4°C by mild rocking with an anti-Folr1 rabbit polyclonal antibody (GenScript, custom-made; 20 μg of IgG per 100 μl of bead suspension) chemically cross-linked to protein G-agarose beads (11719416001, Roche). Beads were re-suspended in 2× protein loading buffer containing 10 mM DTT and incubated for 10 min at 80°C.

Samples were separated on 10% polyacrylamide gels and immunoblotted with anti-C-cadherin (6B6, Developmental Studies Hybridoma Bank; 1:100), anti-β-catenin (AB0095-200, Sicgen; 1:500) and anti-Folr1 antibodies followed by HRP-conjugated anti-mouse and anti-goat secondary antibodies incubation (Jackson ImmunoResearch, 515-035-003 and 705-035-003, respectively) and visualization with enhanced chemiluminescence (ECL2; 80196, Pierce).

### Measurement of folate levels by ELISA assay

Stage 12.5–25 embryos were partially de-jellied by cysteine treatment and samples were weighed, followed by cell lysis and homogenization with 0.5% Triton X-100. Samples were centrifuged at 13,000 *g* and supernatants were loaded onto ELISA plates. Detection of folate level was performed



according to instructions of the folate receptor binding-based Enzyme Immunoassay Kit (7525-300, Monobind) for quantitative determination of folate in biological samples based on the capacity of folate to bind to the folate receptor.

### Immunohistochemistry

Stage 14–18 and 21–23 embryos were fixed for 30 min at 23°C with freshly made 2% trichloroacetic acid (TCA) or 4% paraformaldehyde and processed for immunostaining as previously described (Belgacem and Borodinsky, 2011, 2015; Borodinsky et al., 2004; Swapna and Borodinsky, 2012) with modifications and by using standard protocols of paraffin embedding and sectioning (Tu and Borodinsky, 2014) excluding the permeabilization step with Triton X-100. Tween-20 was used in blocking, antibody and washing solutions for Fnlr1 immunostaining because stronger detergents have been reported to result in artificial redistribution of glycosyl-phosphatidyl-inositol-anchored proteins (Heffer-Laue et al., 2007). Incubations with primary and secondary antibodies were carried out overnight at 4°C and for 2 h at 23°C, respectively. Primary antibodies used were: anti-Fnlr1 (custom-made by GenScript; 1:400), anti-C-cadherin (6B6, Developmental Studies Hybridoma Bank; 1:50), anti- $\beta$ -tubulin (E7, Developmental Studies Hybridoma Bank; 1:300), anti-E-cadherin (5D3, Developmental Studies Hybridoma Bank; 1:100), anti-GFP (GFP-1020, Aves Labs; 1:500), anti-Sox2 (AF2018, R&D Systems; 1:300), anti-m-Cherry (ab 167453, Abcam; 1:500). Antigen retrieval was performed by microwaving samples in 0.05% citraconic anhydride, pH 7.4 (Namimatsu et al., 2005). Briefly, a rack with slides was placed in a 200 ml glass container covered with plastic wrap, boiled for 15 s at maximum power (1200 W) followed by 3 min wait in hot buffer. Slides were washed twice in PBS for 5 min per wash. Further processing starting with a blocking step with 1% bovine serum albumin was carried out using the SNAP i.d. 2.0 System for immunohistochemistry (SNAP2, Millipore).

### Fnlr1 knockdown

Two-cell-stage embryos were bilaterally injected with 4–10 nl of 1 mM Fnlr1-morpholinos, Fnlr1-MO1 and Fnlr1-MO2 (MO oligo sequence written from 5' to 3' and complementary to folate receptor: Fnlr1-MO1, GGCCCCCGTAACATGGTTACAAGC; Fnlr1-MO2, AATATGGCAC GAGTCGCAACCCACA). Controls were sibling embryos injected with standard control morpholino (CMO, CCTCTTACCTCAGTTACAA TTTATA). Morpholinos were injected along with dextran-Alexa-Fluor conjugates or GFP mRNA to assure permanency of the MO reporter after TCA fixation.

Rescue experiments were implemented by expressing Fnlr1-MO1-resistant *Xenopus laevis* *fnlr1* mRNA, lacking 3' UTR, with 5' UTR substituted for gcc acc sequence (Kozak, 1987a,b) and with a number of wobble mutations in coding region (MO-resistant *fnlr1*-RNA: ... gcc acc atg ctt aga gga gct ctc; wt-*fnlr1*-RNA: ... g ctt gta acc atg tta cgg ggg gcc...) or by incubating embryos with 150  $\mu$ M folinic acid. mRNA was synthesized as previously described (Belgacem and Borodinsky, 2011; Borodinsky et al., 2004; Swapna and Borodinsky, 2012) using the *Xenopus laevis* *fnlr1* template (XGC African clawed frog *fnlr1* cDNA, Clone ID: 7012141, Open Biosystems, Thermo Fisher Scientific), subcloned into pCS2+ vector. Mutations were carried out using a site-directed mutagenesis kit (200515, Agilent Technologies; Swapna and Borodinsky, 2012) and PCR reaction to render Fnlr1-MO1-resistant mRNA. Two hundred and fifty pg *fnlr1* mRNA were bilaterally microinjected into two-cell-stage embryos or co-injected with specific MOs. We also designed morpholino-insensitive or front-tagged *fnlr1* (flag-*fnlr1*) and morpholino-sensitive or back-tagged *fnlr1* (*fnlr1*-flag) constructs by subcloning *Xenopus laevis* *fnlr1* into flag-pCS2+ plasmid (Addgene plasmid #16331, deposited by Peter Klein). Another morpholino-sensitive construct was obtained by annealing synthesized Fnlr1-MO1 anti-sense and sense 5'-GCTTGTAACCATGTTC GGGGGGGCC-3' oligonucleotides inserted in front of the flag-*fnlr1* (sense-flag-*fnlr1*). Seven hundred pg of Fnlr1-MO1-resistant *Xenopus laevis* *fnlr1* mRNA were injected in one blastomere of two-cell-stage embryos to overexpress *Xenopus* Fnlr1 unilaterally.

Quantitative assessment of Fnlr1 knockdown by Fnlr1-MO was achieved by measuring the area labeled by Fnlr1 immunostaining in the medial neural plate cell apical surface in sectioned stage 14.5–17 embryos unilaterally

injected with Fnlr1-MO or CMO after uniform thresholding of labeled images with NIS Elements software (Nikon). Measurements were carried out on the apical surface of three consecutive wild-type and three paired Fnlr1-MO- or CMO-containing medial neural plate cells from the midline in ten embryos per group in 42 sections.

Quantitative assessment of C-cadherin-containing vesicles ( $>0.5 \mu$ m) and endosomes (Eea1 immunopositive, 0.2–3  $\mu$ m) was performed by thresholding immunolabeled transverse sections of the medial neural plate followed by counting stained vesicles with NIS Elements software (Nikon). Samples were from stage 15.5–16 embryos unilaterally injected with Fnlr1-MO and CMO in single blastomeres at the two-cell stage. Measurements were performed in three consecutive Fnlr1-MO- and three paired CMO-containing medial neural plate cells from the midline in 18 sections from five embryos.

### Targeted Fnlr1 knockdown in neural and non-neural tissues

Targeting of Fnlr1-MO to neural or non-neural tissues was based on cell fate maps (Moody, 1987). For microinjections, embryos were placed in 6% Ficoll in 0.1 $\times$ MMR. To target the neural plate, 3.6–6 pmol Fnlr1-MO or CMO were injected into the dorsal animal blastomere at the eight-cell stage, or dorsal medial and dorsal lateral animal blastomeres at the 16-cell stage, 1.8–3 pmol per blastomere. To target either medial or lateral neural plate, 1.8–3 pmol of Fnlr1-MO was injected into the dorsal medial or dorsal lateral animal blastomere, respectively, at the 16-cell stage. To target the mesoderm, Fnlr1-MO was injected into the ventral medial animal, dorsal medial vegetal, ventral medial vegetal and ventral lateral vegetal blastomeres at the 16-cell stage, 3 pmol per blastomere. To target the non-neural ectoderm, the ventral lateral animal blastomere at the 16-cell stage was injected with 3 pmol Fnlr1-MO.

### Measurement of neural plate cell apical constriction and cell divisions in live embryos

Two-cell-stage embryos were bilaterally injected with membrane-GFP (pCAG-mGFP, Addgene plasmid # 14757 deposited by Connie Cepko; Matsuda and Cepko, 2007) and unilaterally injected with 10 pmol Fnlr1-MO or CMO per cell along with Alexa 594-conjugated dextran. The rate of apical constriction was analyzed by time-lapse recordings of neurulating embryos over a 1 h period (stage 15–15.5 to 16.5–17) with an acquisition rate of 1 frame/5 min. The surface of medial neural plate cells was measured over time in CMO, Fnlr1-MO-containing and contralateral wild-type cells by creating a region of interest outlining cell boundaries and using NIS-Elements software (Nikon). The total number of cells analyzed was 113 and 115 in CMO- and Fnlr1-MO-injected embryos, respectively,  $n=5$  embryos for each group.

### Measurement of actin dynamics

Two-cell-stage embryos were bilaterally injected with 800 pg mCherry-tagged utrobin mRNA (mCherry-UtrCH, Addgene plasmid #26740, deposited by William Bement; Burkel et al., 2007) and unilaterally injected with 10 pmol Fnlr1-MO per cell along with Alexa 647-conjugated dextran. Medial neural plates of embryos at stage 14–14.5 were imaged for 15 min at 30–55 s intervals using 60 $\times$  objective and z-stack confocal imaging (Sweptfield confocal, Nikon). Fluorescence intensity profiles across cell-cell borders were measured at each time frame on maximum intensity projections using a 2.3–3.5  $\mu$ m stripe (NIS Elements software, Nikon). Intensity profile peaks were fitted with Gauss function in R software following background subtraction. Average Gaussian's width at 50% height was used as a parameter describing F-actin distribution at cell-cell borders in Fnlr1-MO-containing and wild-type medial neural plate cells. Standard deviation of Gaussian's amplitude normalized to amplitude median during 15-min recordings was used to measure dynamics in F-actin accumulation in cell-cell borders. The number of cell borders analyzed was 28 in each group, wild-type and Fnlr1-MO-containing cells,  $n=7$  embryos.

### Pharmacological inhibition of folate action

Neural plate stage embryos (from stage 13 to stage 20) were incubated with 0.1–1500  $\mu$ M methotrexate (MTX), 0.1–300  $\mu$ M MTX-ester, 0.1–100  $\mu$ M pyrimethamine and 100–500  $\mu$ M trimetrexate or vehicle only (control, 0.3%

DMSO or saline). Rescue experiments were performed by preincubating embryos with folic or folinic acid (a metabolically active form of folic acid) starting at the two- to four-cell stage. MTX was added at stage 13, corresponding to the beginning of neural plate folding and neural tube formation.

### TUNEL assay

Labeling of apoptotic cells in transverse sections of developing neural plate and tube was carried out according to instructions in the Apoptag-Fluorescein In Situ Apoptosis Detection Kit (S7110, Millipore).

### Data collection and statistics

Numbers of samples analyzed are indicated for each set of experiments. Significance was evaluated using Student's *t*-test or Mann–Whitney U-test (Wilcoxon rank-sum test) and ANOVA. Differences were considered significant when  $P < 0.05$ .

### Acknowledgements

We thank Dr Karen Zito for comments on the manuscript and Dr Sergey Yechikhov for technical advice.

### Competing interests

The authors declare no competing or financial interests.

### Author contributions

O.A.B., O.V. and L.N.B. designed the experiments; O.A.B. and O.V. performed the experiments and analyzed the data; O.A.B. and L.N.B. wrote the manuscript.

### Funding

This work was supported by a Basil O'Connor Starter Scholar Research Award Grant from the March of Dimes Foundation [5-FY09-131]; a Esther A. and Joseph Klingenstein Fund Foundation Award in Neuroscience; the National Science Foundation [1120796]; the National Institute of Neurological Disorders and Stroke [R01NS073055]; and grants from Shriners Hospitals for Children [86500-NCA, 85220-NCA and 85300-NCA to L.N.B.] and a Shriners Hospitals for Children postdoctoral fellowship (84306-NCA to O.A.B.). Deposited in PMC for release after 12 months.

### Supplementary information

Supplementary information available online at <http://dev.biologists.org/lookup/doi/10.1242/dev.137315.supplemental>

### References

- Afman, L. A., Blom, H. J., Van der Put, N. M. J. and Van Straaten, H. W. M. (2003). Homocysteine interference in neurulation: a chick embryo model. *Birth Defects Res. A Clin. Mol. Teratol.* **67**, 421–428.
- Afman, L. A., Blom, H. J., Driittij, M.-J., Brouns, M. R. and van Straaten, H. W. M. (2005). Inhibition of transmethylation disturbs neurulation in chick embryos. *Brain Res. Dev. Brain Res.* **158**, 59–65.
- Antony, A. C. (1992). The biological chemistry of folate receptors. *Blood* **79**, 2807–2820.
- Antony, A. C. (1996). Folate receptors. *Annu. Rev. Nutr.* **16**, 501–521.
- Barber, R. C., Bennett, G. D., Greer, K. A. and Finnell, R. H. (1999). Expression patterns of folate binding proteins one and two in the developing mouse embryo. *Mol. Genet. Metab.* **66**, 31–39.
- Belgacem, Y. H. and Borodinsky, L. N. (2011). Sonic hedgehog signaling is decoded by calcium spike activity in the developing spinal cord. *Proc. Natl. Acad. Sci. USA* **108**, 4482–4487.
- Belgacem, Y. H. and Borodinsky, L. N. (2015). Inversion of Sonic hedgehog action on its canonical pathway by electrical activity. *Proc. Natl. Acad. Sci. USA* **112**, 4140–4145.
- Blom, H. J., Shaw, G. M., den Heijer, M. and Finnell, R. H. (2006). Neural tube defects and folate: case far from closed. *Nat. Rev. Neurosci.* **7**, 724–731.
- Borodinsky, L. N., Root, C. M., Cronin, J. A., Sann, S. B., Gu, X. and Spitzer, N. C. (2004). Activity-dependent homeostatic specification of transmitter expression in embryonic neurons. *Nature* **429**, 523–530.
- Burkel, B. M., von Dassow, G. and Bement, W. M. (2007). Versatile fluorescent probes for actin filaments based on the actin-binding domain of utrophin. *Cell Motil. Cytoskeleton* **64**, 822–832.
- Chen, Z., Karaplis, A. C., Ackerman, S. L., Pogribny, I. P., Melnyk, S., Lussier-Cacan, S., Chen, M. F., Pai, A., John, S. W., Smith, R. S. et al. (2001). Mice deficient in methylenetetrahydrofolate reductase exhibit hyperhomocysteinemia and decreased methylation capacity, with neuropathology and aortic lipid deposition. *Hum. Mol. Genet.* **10**, 433–443.
- Colas, J.-F. and Schoenwolf, G. C. (2001). Towards a cellular and molecular understanding of neurulation. *Dev. Dyn.* **221**, 117–145.
- Davidson, L. A. and Keller, R. E. (1999). Neural tube closure in *Xenopus laevis* involves medial migration, directed protrusive activity, cell intercalation and convergent extension. *Development* **126**, 4547–4556.
- Detrait, E. R., George, T. M., Etchevers, H. C., Gilbert, J. R., Vekemans, M. and Speer, M. C. (2005). Human neural tube defects: developmental biology, epidemiology, and genetics. *Neurotoxicol. Teratol.* **27**, 515–524.
- Elwood, P. C. (1989). Molecular cloning and characterization of the human folate-binding protein cDNA from placenta and malignant tissue culture (KB) cells. *J. Biol. Chem.* **264**, 14893–14901.
- Eom, D. S., Amarnath, S., Fogel, J. L. and Agarwala, S. (2011). Bone morphogenetic proteins regulate neural tube closure by interacting with the apical-basal polarity pathway. *Development* **138**, 3179–3188.
- Finnell, R. H., Spiegelstein, O., Wlodarczyk, B., Triplett, A., Pogribny, I. P., Melnyk, S. and James, J. S. (2002). DNA methylation in Foltb1 knockout mice supplemented with folic acid during gestation. *J. Nutr.* **132**, 2457S–2461S.
- Giroto, F., Scott, L., Avshalomov, Y., Harris, J., Iannattone, S., Drummond-Main, C., Tobias, R., Bello-Espinosa, L., Rho, J. M., Davidsen, J. et al. (2013). High dose folic acid supplementation of rats alters synaptic transmission and seizure susceptibility in offspring. *Sci. Rep.* **3**, 1465.
- Grem, J. L., Voeller, D. M., Geoffroy, F., Horak, E., Johnston, P. G. and Allegra, C. J. (1994). Determinants of trimetrexate lethality in human colon cancer cells. *Br. J. Cancer* **70**, 1075–1084.
- Haigo, S. L., Hildebrand, J. D., Harland, R. M. and Wallingford, J. B. (2003). Shroom induces apical constriction and is required for hinge-point formation during neural tube closure. *Curr. Biol.* **13**, 2125–2137.
- Harris, W. A. and Hartenstein, V. (1991). Neuronal determination without cell division in *Xenopus* embryos. *Neuron* **6**, 499–515.
- Heffer-Laue, M., Viljetic, B., Vajn, K., Schnaar, R. L. and Laue, G. (2007). Effects of detergents on the redistribution of gangliosides and GPI-anchored proteins in brain tissue sections. *J. Histochem. Cytochem.* **55**, 805–812.
- Hensey, C. and Gautier, J. (1998). Programmed cell death during *Xenopus* development: a spatio-temporal analysis. *Dev. Biol.* **203**, 36–48.
- Hildebrand, J. D. and Soriano, P. (1999). Shroom, a PDZ domain-containing actin-binding protein, is required for neural tube morphogenesis in mice. *Cell* **99**, 485–497.
- Holm, J., Hansen, S. I., Hoier-Madsen, M. and Bostad, L. (1991). High-affinity folate binding in human choroid plexus. Characterization of radioligand binding, immunoreactivity, molecular heterogeneity and hydrophobic domain of the binding protein. *Biochem. J.* **280**, 267–271.
- Hook, K. E., Nelson, J. M., Roberts, B. J., Griswold, D. P. and Leopold, W. R. (1986). Cell cycle effects of trimetrexate (CI-898). *Cancer Chemother. Pharmacol.* **16**, 116–120.
- Iskandar, B. J., Rizk, E., Meier, B., Hariharan, N., Bottiglieri, T., Finnell, R. H., Jarrard, D. F., Banerjee, R. V., Skene, J. H., Nelson, A. et al. (2010). Folate regulation of axonal regeneration in the rodent central nervous system through DNA methylation. *J. Clin. Invest.* **120**, 1603–1616.
- Jarrett, O., Stow, J. L., Yap, A. S. and Key, B. (2002). Dynamin-dependent endocytosis is necessary for convergent-extension movements in *Xenopus* animal cap explants. *Int. J. Dev. Biol.* **46**, 467–473.
- Jolivet, J., Cowan, K. H., Curt, G. A., Clendeninn, N. J. and Chabner, B. A. (1983). The pharmacology and clinical use of methotrexate. *N. Engl. J. Med.* **309**, 1094–1104.
- Kee, N., Wilson, N., De Vries, M., Bradford, D., Key, B. and Cooper, H. M. (2008). Neogenin and RGMa control neural tube closure and neuroepithelial morphology by regulating cell polarity. *J. Neurosci.* **28**, 12643–12653.
- Keller, R., Shih, J., Sater, A. K. and Moreno, C. (1992). Planar induction of convergence and extension of the neural plate by the organizer of *Xenopus*. *Dev. Dyn.* **193**, 218–234.
- Klein, S. L., Strausberg, R. L., Wagner, L., Pontius, J., Clifton, S. W. and Richardson, P. (2002). Genetic and genomic tools for *Xenopus* research: the NIH *Xenopus* initiative. *Dev. Dyn.* **225**, 384–391.
- Koch, M. C., Stegmann, K., Ziegler, A., Schröter, B. and Ermert, A. (1998). Evaluation of the MTHFR C677T allele and the MTHFR gene locus in a German spina bifida population. *Eur. J. Pediatr.* **157**, 487–492.
- Kozak, M. (1987a). An analysis of 5'-noncoding sequences from 699 vertebrate messenger RNAs. *Nucleic Acids Res.* **15**, 8125–8148.
- Kozak, M. (1987b). At least six nucleotides preceding the AUG initiator codon enhance translation in mammalian cells. *J. Mol. Biol.* **196**, 947–950.
- Lee, J.-Y. and Harland, R. M. (2010). Endocytosis is required for efficient apical constriction during *Xenopus* gastrulation. *Curr. Biol.* **20**, 253–258.
- Matsuda, T. and Cepko, C. L. (2007). Controlled expression of transgenes introduced by in vivo electroporation. *Proc. Natl. Acad. Sci. USA* **104**, 1027–1032.
- Meuli, M. and Moehrlen, U. (2014). Fetal surgery for myelomeningocele is effective: a critical look at the whys. *Pediatr. Surg. Int.* **30**, 689–697.
- Moody, S. A. (1987). Fates of the blastomeres of the 16-cell stage *Xenopus* embryo. *Dev. Biol.* **119**, 560–578.
- Morita, H., Nandadasa, S., Yamamoto, T. S., Terasaka-Iioka, C., Wylie, C. and Ueno, N. (2010). Nectin-2 and N-cadherin interact through extracellular domains

- and induce apical accumulation of F-actin in apical constriction of *Xenopus* neural tube morphogenesis. *Development* **137**, 1315-1325.
- Mornet, E., Muller, F., Lenois-Furet, A., Delezoide, A. L., Col, J. Y., Simon-Bouy, B. and Serre, J.-L. (1997). Screening of the C677T mutation on the methylenetetrahydrofolate reductase gene in French patients with neural tube defects. *Hum. Genet.* **100**, 512-514.
- Moury, J. D. and Schoenwolf, G. C. (1995). Cooperative model of epithelial shaping and bending during avian neurulation: autonomous movements of the neural plate, autonomous movements of the epidermis, and interactions in the neural plate/epidermis transition zone. *Dev. Dyn.* **204**, 323-337.
- MRC Vitamin Study Research Group (1991). Prevention of neural tube defects: results of the medical research council vitamin study. *Lancet* **338**, 131-137.
- Mu, F.-T., Callaghan, J. M., Steele-Mortimer, O., Stenmark, H., Parton, R. G., Campbell, P. L., McCluskey, J., Yeo, J.-P., Tock, E. P. and Toh, B.-H. (1995). EEA1, an early endosome-associated protein. EEA1 is a conserved alpha-helical peripheral membrane protein flanked by cysteine "fingers" and contains a calmodulin-binding IQ motif. *J. Biol. Chem.* **270**, 13503-13511.
- Namimatsu, S., Ghazizadeh, M. and Sugisaki, Y. (2005). Reversing the effects of formalin fixation with citraconic anhydride and heat: a universal antigen retrieval method. *J. Histochem. Cytochem.* **53**, 3-11.
- Nandadasa, S., Tao, Q., Menon, N. R., Heasman, J. and Wylie, C. (2009). N- and E-cadherins in *Xenopus* are specifically required in the neural and non-neural ectoderm, respectively, for F-actin assembly and morphogenetic movements. *Development* **136**, 1327-1338.
- Nieuwkoop, P. D. and Faber, J. (1994). *Normal Table of *Xenopus Laevis* (Daudin): A Systematical and Chronological Survey of the Development from the Fertilized Egg Till the End of Metamorphosis*. New York: Garland Pub.
- Nishimura, T. and Takeichi, M. (2008). Shroom3-mediated recruitment of Rho kinases to the apical cell junctions regulates epithelial and neuroepithelial planar remodeling. *Development* **135**, 1493-1502.
- Nishimura, T. and Takeichi, M. (2009). Remodeling of the adherens junctions during morphogenesis. *Curr. Top. Dev. Biol.* **89**, 33-54.
- O'Byrne, M. R., Au, K. S., Morrison, A. C., Lin, J.-I., Fletcher, J. M., Ostermaier, K. K., Tyerman, G. H., Doebel, S. and Northrup, H. (2010). Association of folate receptor (FOLR1, FOLR2, FOLR3) and reduced folate carrier (SLC19A1) genes with meningomyelocele. *Birth Defects Res. A Clin. Mol. Teratol.* **88**, 689-694.
- Ossipova, O., Kim, K., Lake, B. B., Itoh, K., Ioannou, A. and Sokol, S. Y. (2014). Role of Rab11 in planar cell polarity and apical constriction during vertebrate neural tube closure. *Nat. Commun.* **5**, 3734.
- Papapetrou, C., Lynch, S. A., Burn, J. and Edwards, Y. H. (1996). Methylenetetrahydrofolate reductase and neural tube defects. *Lancet* **348**, 58.
- Piedrahita, J. A., Oetama, B., Bennett, G. D., van Waes, J., Kamen, B. A., Richardson, J., Lacey, S. W., Anderson, R. G. W. and Finnell, R. H. (1999). Mice lacking the folic acid-binding protein Folbp1 are defective in early embryonic development. *Nat. Genet.* **23**, 228-232.
- Pitkin, R. M. (2007). Folate and neural tube defects. *Am. J. Clin. Nutr.* **85**, 285S-288S.
- Prasad, P. D., Ramamoorthy, S., Moe, A. J., Smith, C. H., Leibach, F. H. and Ganapathy, V. (1994). Selective expression of the high-affinity isoform of the folate receptor (FR-alpha) in the human placental syncytiotrophoblast and choriocarcinoma cells. *Biochim. Biophys. Acta* **1223**, 71-75.
- Ramaekers, V. T., Rothenberg, S. P., Sequeira, J. M., Opladen, T., Blau, N., Quadros, E. V. and Selhub, J. (2005). Autoantibodies to folate receptors in the cerebral folate deficiency syndrome. *N. Engl. J. Med.* **352**, 1985-1991.
- Saito, H., Ishibashi, M., Nakano, H. and Shiota, K. (2003). Spatial and temporal expression of folate-binding protein 1 (Fbp1) is closely associated with anterior neural tube closure in mice. *Dev. Dyn.* **226**, 112-117.
- Schoenwolf, G. C. (1988). Microsurgical analyses of avian neurulation: separation of medial and lateral tissues. *J. Comp. Neurol.* **276**, 498-507.
- Schoenwolf, G. C., Everaert, S., Bortier, H. and Vakaet, L. (1989). Neural plate- and neural tube-forming potential of isolated epiblast areas in avian embryos. *Anat. Embryol. (Berl)* **179**, 541-549.
- Selhub, J. and Franklin, W. A. (1984). The folate-binding protein of rat kidney. Purification, properties, and cellular distribution. *J. Biol. Chem.* **259**, 6601-6606.
- Sequeira, J. M., Desai, A., Berrocal-Zaragoza, M. I., Murphy, M. M., Fernandez-Ballart, J. D. and Quadros, E. V. (2016). Exposure to folate receptor alpha antibodies during gestation and weaning leads to severe behavioral deficits in rats: a pilot study. *PLoS ONE* **11**, e0152249.
- Sirotnak, F. M. and Tolner, B. (1999). Carrier-mediated membrane transport of folates in mammalian cells. *Annu. Rev. Nutr.* **19**, 91-122.
- Smithells, R. W., Sheppard, S. and Schorah, C. J. (1976). Vitamin deficiencies and neural tube defects. *Arch. Dis. Child.* **51**, 944-950.
- Speer, M. C., Worley, G., Mackey, J. F., Melvin, E., Oakes, W. J. and George, T. M. (1997). The thermolabile variant of methylenetetrahydrofolate reductase (MTHFR) is not a major risk factor for neural tube defect in American Caucasians. The NTD Collaborative Group. *Neurogenetics* **1**, 149-150.
- Spiegelstein, O., Mitchell, L. E., Merriweather, M. Y., Wicker, N. J., Zhang, Q., Lammer, E. J. and Finnell, R. H. (2004). Embryonic development of folate binding protein-1 (Folbp1) knockout mice: Effects of the chemical form, dose, and timing of maternal folate supplementation. *Dev. Dyn.* **231**, 221-231.
- Sugimoto, K., Okabayashi, K., Sedohara, A., Hayata, T. and Asashima, M. (2007). The role of XBTg2 in *Xenopus* neural development. *Dev. Neurosci.* **29**, 468-479.
- Swanson, D. A., Liu, M.-L., Baker, P. J., Garrett, L., Stitzel, M., Wu, J., Harris, M., Banerjee, R., Shane, B. and Brody, L. C. (2001). Targeted disruption of the methionine synthase gene in mice. *Mol. Cell. Biol.* **21**, 1058-1065.
- Swapna, I. and Borodinsky, L. N. (2012). Interplay between electrical activity and bone morphogenetic protein signaling regulates spinal neuron differentiation. *Proc. Natl. Acad. Sci. USA* **109**, 16336-16341.
- Tu, M. K. and Borodinsky, L. N. (2014). Spontaneous calcium transients manifest in the regenerating muscle and are necessary for skeletal muscle replenishment. *Cell Calcium* **56**, 34-41.
- van der Put, N. M. J., Steegers-Theunissen, R. P., Frosst, P., Trijbels, F. J., Eskes, T. K., van den Heuvel, L. P., Mariman, E. C., den Heyer, M., Rozen, R. and Blom, H. J. (1995). Mutated methylenetetrahydrofolate reductase as a risk factor for spina bifida. *Lancet* **346**, 1070-1071.
- van der Put, N. M. J., van den Heuvel, L. P., Steegers-Theunissen, R. P., Trijbels, F. J., Eskes, T. K., Mariman, E. C., den Heyer, M. and Blom, H. J. (1996). Decreased methylene tetrahydrofolate reductase activity due to the 677C→T mutation in families with spina bifida offspring. *J. Mol. Med. (Berl.)* **74**, 691-694.
- Wallingford, J. B. and Harland, R. M. (2002). Neural tube closure requires Dishevelled-dependent convergent extension of the midline. *Development* **129**, 5815-5825.
- Wallingford, J. B., Niswander, L. A., Shaw, G. M. and Finnell, R. H. (2013). The continuing challenge of understanding, preventing, and treating neural tube defects. *Science* **339**, 1222-1223.
- Watanabe, M., Osada, J., Aratani, Y., Kluckman, K., Reddick, R., Malinow, M. R. and Maeda, N. (1995). Mice deficient in cystathionine beta-synthase: animal models for mild and severe homocyst(e)inemia. *Proc. Natl. Acad. Sci. USA* **92**, 1585-1589.
- West, J. J. and Harris, T. J. C. (2016). Cadherin trafficking for tissue morphogenesis: control and consequences. *Traffic* **17**, 1233-1243.
- Wilcken, D. E. L. and Wang, X. L. (1996). Relevance to spina bifida of mutated methylenetetrahydrofolate reductase. *Lancet* **347**, 340.
- Zimmerman, J., Selhub, J. and Rosenberg, I. H. (1987). Competitive inhibition of folate absorption by dihydrofolate reductase inhibitors, trimethoprim and pyrimethamine. *Am. J. Clin. Nutr.* **46**, 518-522.



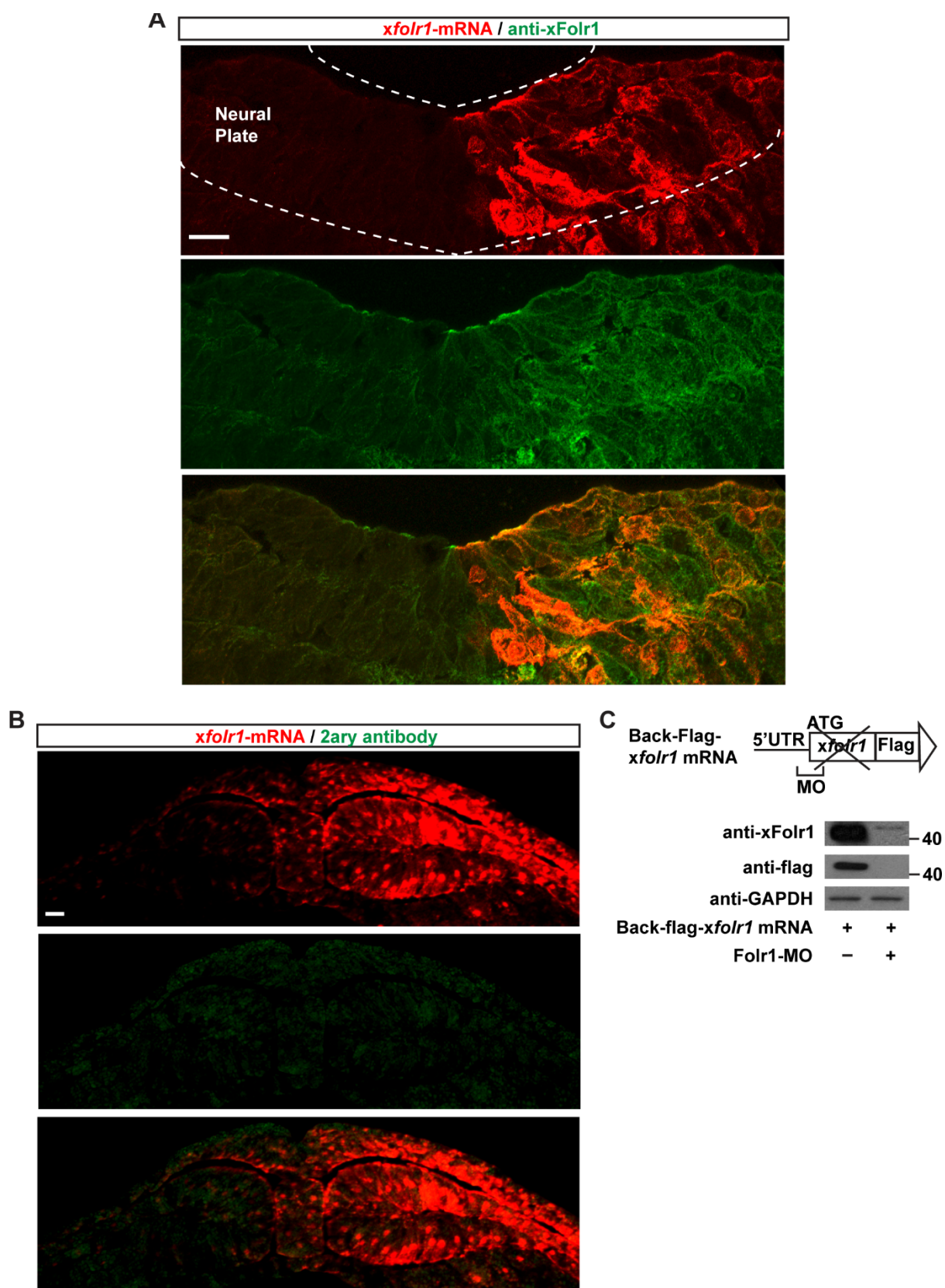


**Fig. S1. Specificity of *Xenopus* folate receptor 1 antibody.** (A,B) Two-cell-stage embryos were unilaterally injected with 700 pg *xfolr1* mRNA+GFP mRNA (A) or Alexa Fluor 594-dextran conjugate (B), paraffin-sectioned and processed for xFolr1 immunostaining with (A) or without (B) Folr1 primary antibody added. Scale bar: 20  $\mu$ m. (C) Schematic of construct to demonstrate specificity of xFolr1 antibody and representative Western blot from whole cell homogenates from embryos injected at the 2-cell stage with the indicated constructs. xFolr1: *Xenopus laevis* folate receptor 1, Folr1-MO: xFolr1-targeted translation blocking-morpholino.

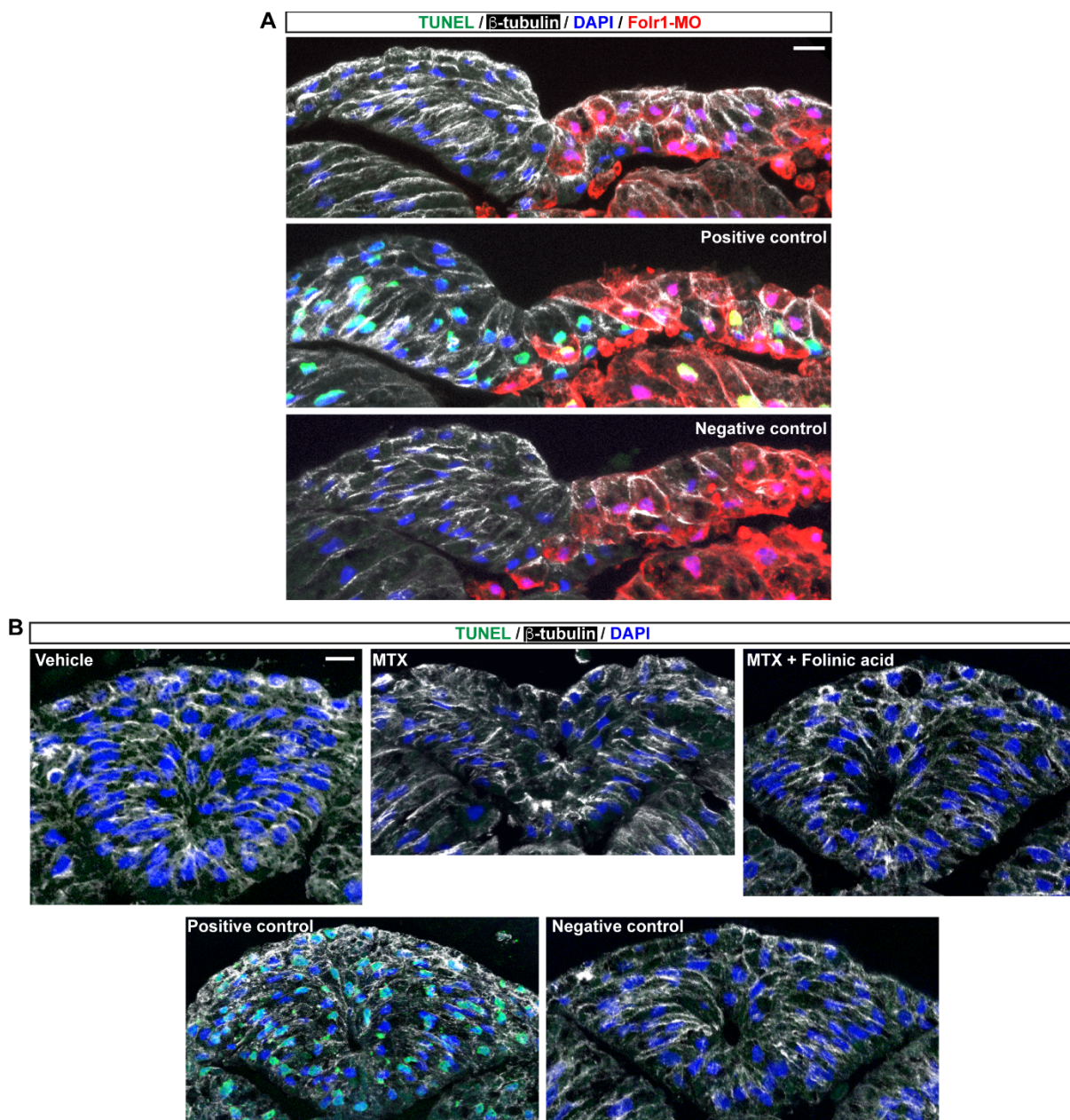


**Fig. S2. Folr1-MO or methotrexate does not induce apoptosis of neural plate cells during neurulation.** (A) Two-cell-stage embryos were unilaterally injected with 10 pmol folate receptor 1 morpholino (Folr1-MO) and Alexa 594-conjugated dextran and grown until neural plate stage 17 (18.75 hpf). (B) Early neural plate stage embryos (stage 13, 14.75 hpf) were incubated in the absence (Control) or presence of 1-1.5 mM methotrexate (MTX) until closure of the neural tube in controls (stage 20, 21.75 hpf). (A,B) Embryos were then processed for TUNEL assay, immunostaining for  $\beta$ -tubulin and nuclear labeling with DAPI. Shown are representative transverse sections of neural tissue from aforementioned embryos. Positive control is a sample treated with DNase; negative control is a sample in which no labeling enzyme (Terminal Deoxynucleotidyl Transferase) was added. Scale bars: 20  $\mu$ m.



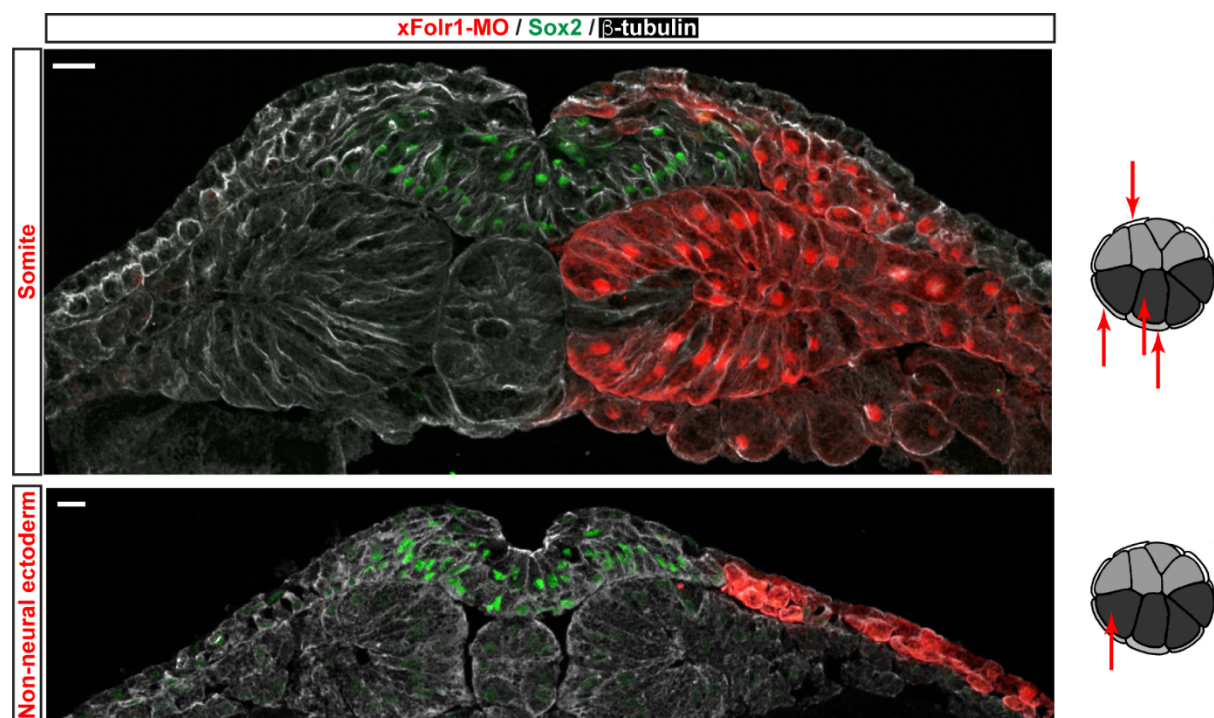


**Fig. S3. Knockdown of folate receptor 1 in mesoderm or non-neural ectoderm does not induce neural tube defects.** Targeted blastomeres of 16-cell-stage embryos were unilaterally microinjected with 3 pmol/cell morpholino against the *Xenopus laevis* Folr1 (Folr1-MO) along with Alexa 594-dextran conjugate in indicated blastomeres (left). Neural plate stage embryos were then sectioned and processed for immunostaining with anti-β-tubulin (grayscale) and Sox2 (green). Red indicates MO-containing cells. Scale bars: 20 μm.

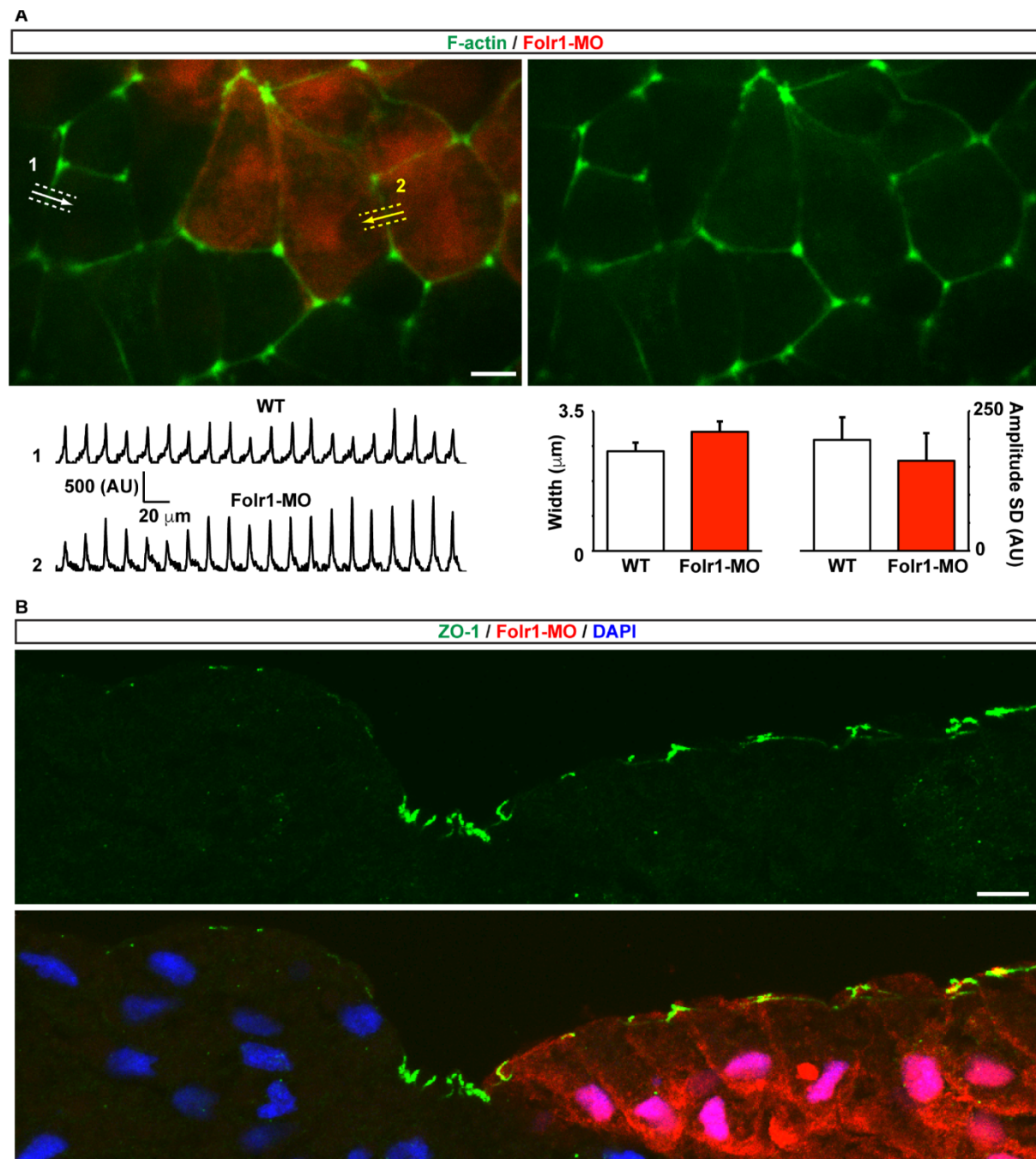


**Fig. S4. Folr1 knockdown does not induce changes in actin dynamics or in overall apicobasal polarity in the folding neural plate.** (A) Two-cell-stage embryos were unilaterally microinjected with Folr1-MO along with Alexa Fluor 594-dextran conjugate (red) and bilaterally injected with mCherry-UtrophinCH (F-actin reporter, green). Superficial medial neural plate was time-lapse imaged from whole embryos at a rate of 1-2 min<sup>-1</sup>. Fluorescence intensity profiles (arrows) across cell-cell borders were measured among wild-type (WT, 1) and Folr1-MO (2) containing cells during 15 min imaging. Scale bar, 10  $\mu$ m. Intensity profiles were fitted with Gauss function using R software after background subtraction. Bar graph shows mean $\pm$ SEM peak width at 50% maximum intensity (left) and standard deviation (SD) of normalized maximum intensity during 15 min recording (right), n: 28 cell-cell borders per group, t-test. (B) Unilateral Folr1-MO-containing neural plate stage embryos were sectioned and processed for immunostaining with anti-ZO-1 (green). Scale bar, 20  $\mu$ m.

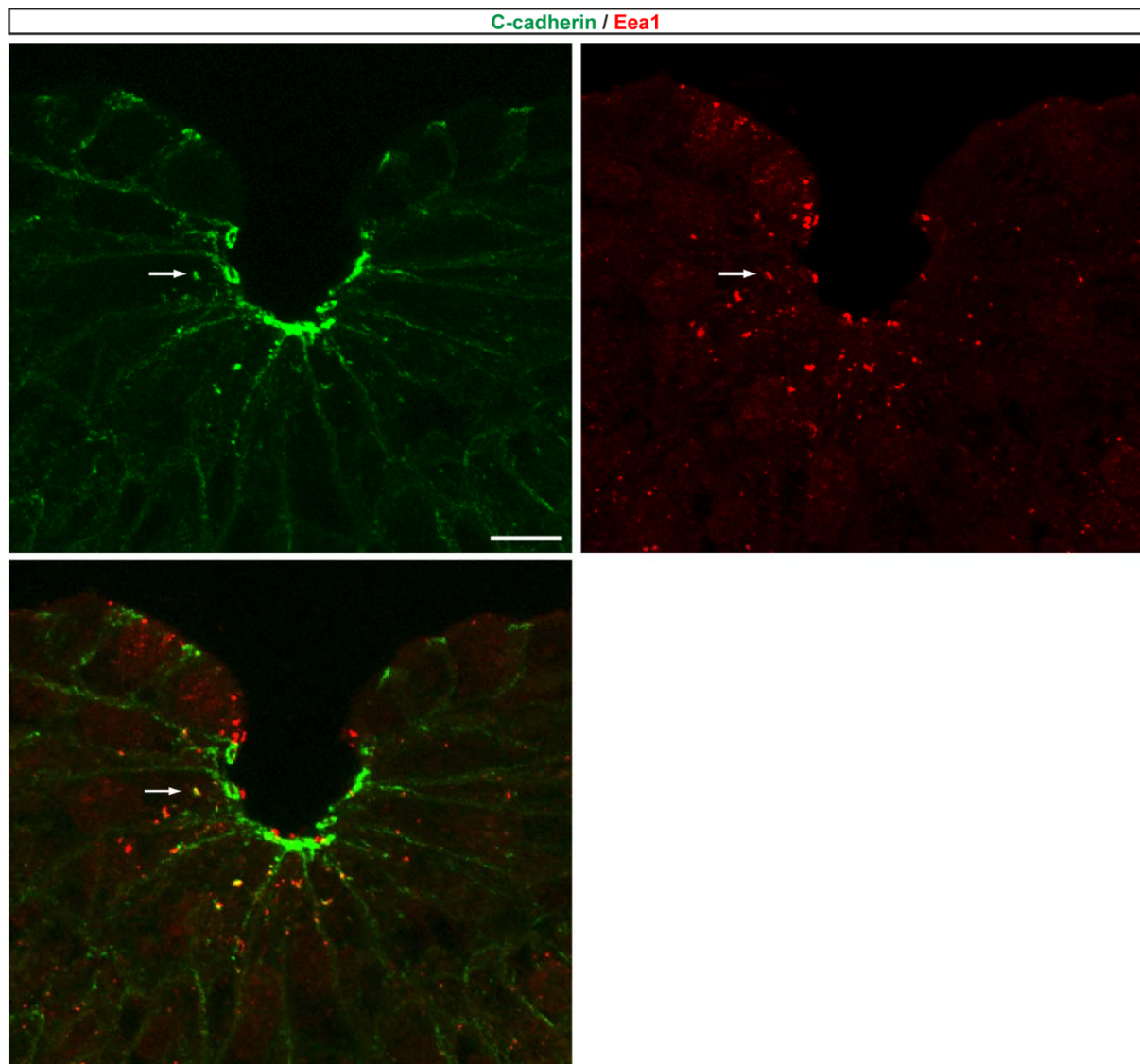
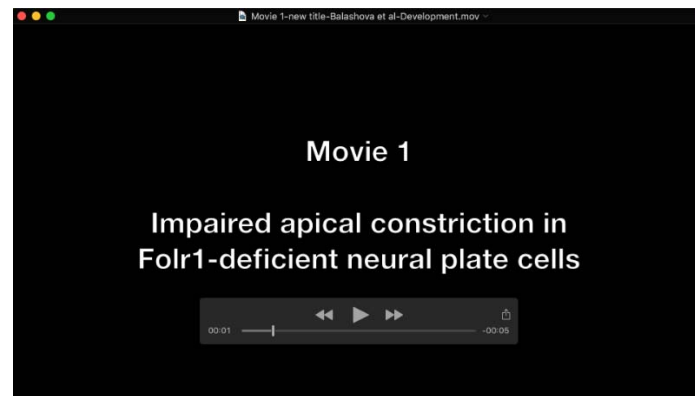
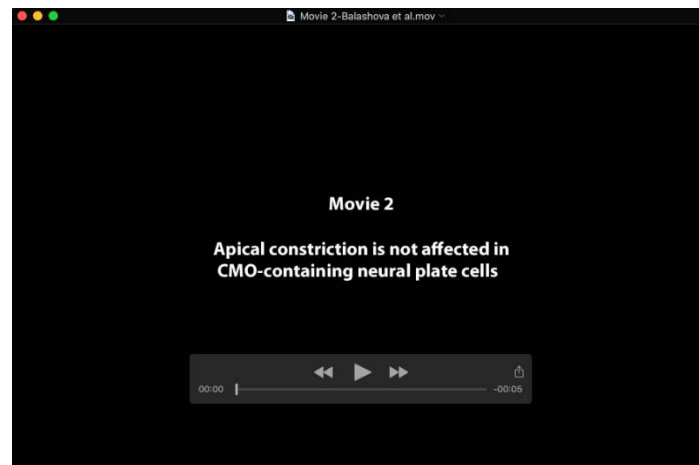


**Fig. S5. Neural plate cell apical constriction is concurrent with endocytosis of C-cadherin.** Neural plate stage embryos were sectioned and processed for immunostaining with anti-C-cadherin (green) and anti-Eea1 (red). Scale bar, 20  $\mu$ m. Arrow points to a C-cadherin-containing endosome.



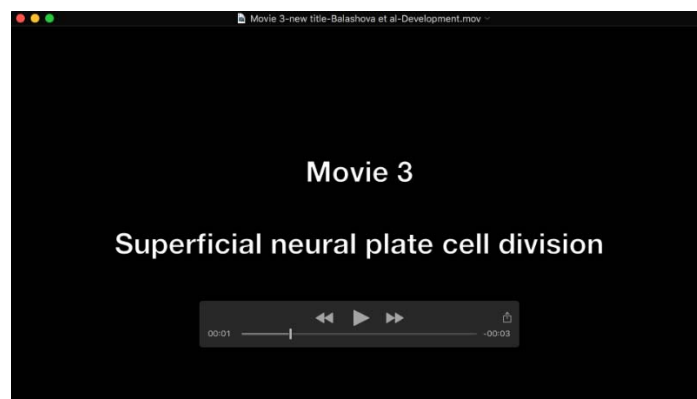


**Movie 1. Impaired apical constriction in Fcrl1-deficient neural plate cells.** Two-cell-stage embryos were bilaterally injected with membrane-GFP (in green) and unilaterally with 10 pmol Fcrl1-MO + AlexaFluor 594-dextran conjugate (in red). Confocal images of the apical neural plate in live embryos at stage 15-15.5 were taken every 5 min. Shown are z-projections of the sequence of time frames during 1 h recording. Note decrease in cell surface, folding of the neural plate and appearance of non-neural ectoderm (relatively big hexagonal cells) towards the end of the movie in the wild-type side (top, green), while neural plate cells containing Fcrl1-MO fail to constrict and the neural plate does not fold (bottom, yellow).



**Movie 2. Apical constriction is not affected in CMO-containing neural plate cells.**

Two-cell-stage embryos were bilaterally injected with membrane-GFP (in green) and unilaterally with 10 pmol CMO + AlexaFluor 594-dextran conjugate (in red). Confocal images of the apical neural plate in live embryos at stage 15-15.5 were taken every 5 min. Shown are z-projections of the sequence of time frames during 1 h recording. Sample realignment was done after 30-min recording to recenter the field of view on the neural plate midline. Note decrease in cell surface and folding of the neural plate in the wild-type (top, green) and CMO-containing neural plate (bottom, yellow).



**Movie 3. Apical neural plate cell division.** Two-cell-stage embryos were bilaterally injected with membrane-GFP (in green) and unilaterally with 10 pmol Folr1-MO + AlexaFluor 594-dextran conjugate (in red). Confocal images of the apical neural plate in live embryos at stage 15-15.5 were taken every 5 min. Shown are z-projections of the sequence of time frames during 25 min recording. Asterisks indicate dividing and daughter cells. Dividing cells were excluded from the measurements of changes in apical cell surface during neural plate folding (Fig. 6). The proportion of dividing apical cells is small during neural plate folding and is similar in wild type and Folr1-deficient cells (see Results for details).